

THE
IIOAB
JOURNAL

VOLUME 9 : NO 4 : NOVEMBER 2017 : ISSN 0976-3104



Institute of Integrative Omics and
Applied Biotechnology Journal

Dear Esteemed Readers, Authors, and Colleagues,

I hope this letter finds you in good health and high spirits. It is my distinct pleasure to address you as the Editor-in-Chief of Integrative Omics and Applied Biotechnology (IIOAB) Journal, a multidisciplinary scientific journal that has always placed a profound emphasis on nurturing the involvement of young scientists and championing the significance of an interdisciplinary approach.

At Integrative Omics and Applied Biotechnology (IIOAB) Journal, we firmly believe in the transformative power of science and innovation, and we recognize that it is the vigor and enthusiasm of young minds that often drive the most groundbreaking discoveries. We actively encourage students, early-career researchers, and scientists to submit their work and engage in meaningful discourse within the pages of our journal. We take pride in providing a platform for these emerging researchers to share their novel ideas and findings with the broader scientific community.

In today's rapidly evolving scientific landscape, it is increasingly evident that the challenges we face require a collaborative and interdisciplinary approach. The most complex problems demand a diverse set of perspectives and expertise. Integrative Omics and Applied Biotechnology (IIOAB) Journal has consistently promoted and celebrated this multidisciplinary ethos. We believe that by crossing traditional disciplinary boundaries, we can unlock new avenues for discovery, innovation, and progress. This philosophy has been at the heart of our journal's mission, and we remain dedicated to publishing research that exemplifies the power of interdisciplinary collaboration.

Our journal continues to serve as a hub for knowledge exchange, providing a platform for researchers from various fields to come together and share their insights, experiences, and research outcomes. The collaborative spirit within our community is truly inspiring, and I am immensely proud of the role that IIOAB journal plays in fostering such partnerships.

As we move forward, I encourage each and every one of you to continue supporting our mission. Whether you are a seasoned researcher, a young scientist embarking on your career, or a reader with a thirst for knowledge, your involvement in our journal is invaluable. By working together and embracing interdisciplinary perspectives, we can address the most pressing challenges facing humanity, from climate change and public health to technological advancements and social issues.

I would like to extend my gratitude to our authors, reviewers, editorial board members, and readers for their unwavering support. Your dedication is what makes IIOAB Journal the thriving scientific community it is today. Together, we will continue to explore the frontiers of knowledge and pioneer new approaches to solving the world's most complex problems.

Thank you for being a part of our journey, and for your commitment to advancing science through the pages of IIOAB Journal.



Yours sincerely,

Vasco Azevedo

Vasco Azevedo, Editor-in-Chief
Integrative Omics and Applied Biotechnology
(IIOAB) Journal



Prof. Vasco Azevedo
Federal University of Minas Gerais
Brazil

Editor-in-Chief

Integrative Omics and Applied Biotechnology (IIOAB) Journal Editorial Board:



Nina Yiannakopoulou
Technological Educational Institute of Athens
Greece



Jyoti Mandlik
Bharati Vidyapeeth University
India



Rajneesh K. Gaur
Department of Biotechnology, Ministry of Science and Technology
India



Swarnalatha P
VIT University
India



Vinay Aroskar
Sterling Biotech Limited
Mumbai, India



Sanjay Kumar Gupta
Indian Institute of Technology
New Delhi, India



Arun Kumar Sangaiah
VIT University
Vellore, India



Sumathi Suresh
Indian Institute of Technology
Bombay, India



Bui Huy Khoi
Industrial University of Ho Chi Minh City
Vietnam



Tetsuji Yamada
Rutgers University
New Jersey, USA



Moustafa Mohamed Sabry Bakry
Plant Protection Research Institute
Giza, Egypt



Rohan Rajapakse
University of Ruhuna
Sri Lanka



Atun RoyChoudhury
Ramky Advanced Centre for Environmental Research
India



N. Arun Kumar
SASTRA University
Thanjavur, India



Bui Phu Nam Anh
Ho Chi Minh Open University
Vietnam



Steven Fernandes
Sahyadri College of Engineering & Management
India

ARTICLE

RELATIONSHIP BETWEEN BCL-2 EXPRESSION AND APOPTOSIS INDEX ON RAT (*RATTUS NORVEGICUS*) MODEL OF PREECLAMPSIA AFTER ADMINISTRATION OF EVOOIrianti Evi^{1*}, Ilyas Syafruddin¹, Rosidah², Salomo Hutahaean¹¹Departement of Biology, University of Sumatera Utara, Medan, INDONESIA²Department of Pharmacy, University of Sumatera Utara, Medan, INDONESIA

ABSTRACT

One cause of preeclampsia is due to an imbalance between antioxidants and free radicals, due to the failure of spiral artery remodeling, resulting in placenta ischemia and hypoxia. The occurring hypoxia mediates mir210 to induce the expression of the antiapoptotic Bcl-2 (B-cell lymphoma-2) target gene that may reduce excessive apoptosis. This study aims to prevent this imbalance by giving extra virgin olive oil (EVOO) rich in tocopherol content (vitamin E). The design of this study is pre- and post-test with control group design in the laboratory. Subject is a female rat, Sprague Dawley strain, weight \pm 200g. The control and treatment groups consisted of a total sample of 25 individuals. Bcl-2 expression increased significantly, especially in the treatment group that received EVOO (P value 0,009). Apoptosis index tended to decrease in treatment group that received low and moderate dose of EVOO, but there was no significance (P value 0.332). Conclusions: EVOO was able to increase Bcl-2 to prevent excessive apoptosis on preeclampsia. It is recommended to examine the expression of p53 or Bax protein to find out which protein regulates apoptotic.

INTRODUCTION

Maternal Mortality Rate (MMR) is an important indicator of public health status. Maternal mortality can be caused by several factors, including bleeding, preeclampsia, and infection [1]. In 2012, Indonesia is still one of the countries in Southeast Asia with the highest MMR, 359 / 100.000 live birth and about 27% of the cause is preeclampsia, about 13,500 persons per year¹. Preeclampsia is a syndrome in early pregnancy, characterized by gestational hypertension and proteinuria (although current diagnosis of preeclampsia does not depend on proteinuria), occurring after 20 weeks of gestation, and is one cause of maternal death [2-4].

One of the major causes of preeclampsia is an imbalance between antioxidants and free radicals, due to the failure of spiral artery remodeling. Failure of spiral artery remodeling results in the placenta having ischemia and hypoxia [5]. The occurring hypoxia mediates m RNA210 to induce the expression of the anti-apoptotic Bcl-2 (B-cell lymphoma-2) target gene to reduce excessive apoptosis [6]. In addition, placental hypoxia with preeclampsia can lead to apoptosis, especially through the intrinsic pathway of mitochondria [7]. Another study revealed, in preeclampsia, there was an increase in index apoptosis [8]. Preeclampsia causes excessive apoptosis and decreased expression of Bcl-2[7]. Another study revealed the increase in apoptosis followed by decreased expression of Bcl-2 and Bcl-xl proteins in severe preeclampsia pregnancies compared to normotensive pregnancies [9]. Therefore, it is necessary to prevent preeclampsia, and one method is by giving antioxidant [10]. One type of antioxidant known is extra virgin olive oil (EVOO), rich in antioxidant content of tocopherol [11].

Another benefit of EVOO is to protect hepatic tissue from damage by oxidation by preventing lipid peroxide activity by increasing the formation of MUFA (monounsaturated fatty acid) and maintaining serum marker enzymes, as well as the activity of hepatic antioxidant enzymes at concentrations close to normal. In addition, the hydrophilic fraction, part of the olive oil proved to be effective in reducing oxidative stress and, in this extra hydrophilic case, it potentially has a direct antioxidant effect on hepatic cells[11]. Other studies have found that eating EVOO three times a day can reduce oxidative stress in the pancreas [12].

Based on the above description, the benefits of EVOO as an antioxidant have been known, but we know of no research on cases of preeclampsia. Based on the consideration of ethics and safety of materials used on mothers and fetuses, difficulty getting volunteers, as well as external factors (e.g., nutrients) that are not easily controlled, it is necessary to model the experimental animals of white rats (*Rattus norvegicus*) in this study[13]. Therefore, we are interested to know the relationship between Bcl-2 expression and apoptosis on placenta cells. The purpose of this research is to know the description of Bcl-2 expression and apoptosis index, as well as the relationship between of them. Hypothesis: The study found an increase in mean expression of Bcl-2 and apoptosis index in placenta after administration of EVOO. Novelty of this research: As far as we know, there is no research about the effect of giving EVOO on Bcl-2 expression on white rat (*Rattus norvegicus*) and its contribution to prevention of oxidative stress occurring in preeclampsia, so it is expected to give knowledge about alternative prevention of preeclampsia.

KEY WORDS

EVOO, preeclampsia, Bcl-2, apoptotic index

Received: 30 April 2018
Accepted: 13 June 2018
Published: 1 July 2018

*Corresponding Author

Email: eviriantfi2015@gmail.com
Tel.: + 62 821 14982353
Fax: + 62 061 4524550

MATERIALS AND METHODS

The location of the research was conducted in the veterinary laboratory of pharmacology department and therapy of Medical Faculty of Padjadjaran University Bandung and Anatomy Pathology Laboratory of Medical Faculty University of Sumatera Utara Medan (permit and implementation of attached study). Before the research was conducted, a permission letter of ethical clearance from the animal research ethics committee of FMIPA USU was issued. The type of research is true experiment done in a laboratory with pre- and post-test design with control group design.

Materials and tools of research at preparation of white female rat (*Rattus norvegicus*) strain of Sparague Dawley counted 25 tails, eight male rats (1: 3 or 4 mating ratio), 8-11 weeks old and body weight \pm 200 gram (addition or a reduction in the weight range of about 10%), mice in healthy condition, marked with the presence of fluff (not standing); the movement is quite agile and does not show physical disability. Given standard AIN93-M food and enough drinks. The implementation of the study was performed by injecting NaCl 6% sterile 3cc daily, starting from 6th to 12th days of pregnancy in subcutaneous and intramuscular to obtain preeclampsia model animals in the treatment group, sleeve or paralon pipe (rat body size) for 30 minutes only once on the 19th day of pregnancy. The required material at the time of the research intervention was EVOO, and the tool used was a non-invasive sphygmomanometer to measure increase in blood pressure. If blood pressure increased after giving treatment, it means the animal's sustained preeclampsia.

The observation of apoptotic cells using DNA-fragmented techniques. The materials used are TUNEL kit, PBS solution pH 7.4, H₂O₂ 3%, DAB (Diamino Benzidine), Peroxidase solution, Mayer Hematoxilen. The tool used a light microscope. Observation of Bcl-2 expression of the required material Tris Buffered Saline (TBS) pH 7.4, Primary TissueTM, peroxide block, Bcl-2 primary antibody Monoclonal Mouse Antibody IgG2B Clone # 625509 (catalog # MAB8272) with species reactivity Human / Mouse / Rat from R & D SYSTEMSbiotechne, PolyVue PlusTM Enhancer, PolyVue PlusTM HRP (Horseradish-peroxidase) reagents, DAB / PlusTM, Mayer Hematoxylin. The tools used are PT Link Dako Epitope Retrieval, Pap pen, cover glass, and microscope. The experimental animals consisted of 5 groups, each group consisting of 5 white rats. The group was divided into the control group (P0), and the treatment consisted of P1: preeclampsia model, P2: preeclampsia model + dosage of EVOO: 0.38 mL / kg BW, P3: preeclampsia model + dosage of EVOO 0.76 mL / kg BW, P4: model preeclampsia + dosage of EVOO 1.52 mL / kg BW. The data collected were analyzed by Anova or Kruskal Wallis statistical test and Spearman correlation.

RESULTS

The results of Bcl-2 expression of placenta tissue can be seen in [Fig. 1] below:

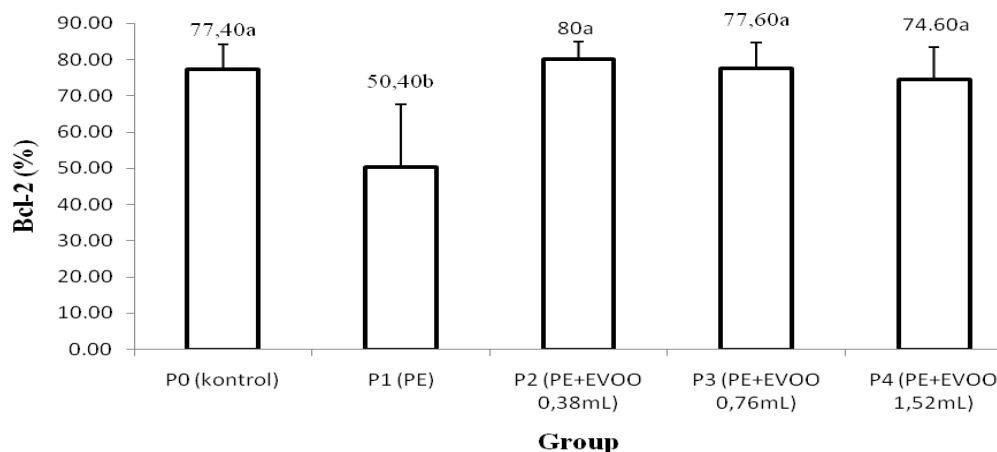


Fig.1: Effect of EVOO on protein expression of Bcl-2 placenta tissue of pregnant white rat. The same small letters show no significance ($P > 0.05$).

Based on [Fig.1], it is known that, after administration of EVOO, there is a significant difference in Bcl-2 protein expression between control and treatment groups (Kruskal Wallis test, $P = 0.020$). In this case, EVOO affects the increased expression of Bcl-2 protein in the treatment group that received it. Increased expression of Bcl-2 protein in the treated group with EVOO was similar to that of control, but not in P1 (group not given EVOO), which was lower. This is evident from Mann Whitney test results; the expression of Bcl-2 protein in P1 was significantly different from other groups. Interestingly, in this study, increased expression of Bcl-2 protein in the P2 group was quite high (strongly positive) in almost all placental tissues compared to the other groups. The P1 group of Bcl-2 protein expression was moderately positive.

Observation of apoptotic cells in the placenta tissue immunohistochemically using TUNEL kit. Apoptotic cells are calculated to determine the apoptosis index. The tissue used was the placenta stored in paraffin blocks. Calculation of apoptosis index was qualitative then converted to semi quantitative based on predetermined criterion [14], the result as shown in [Fig. 2] below:

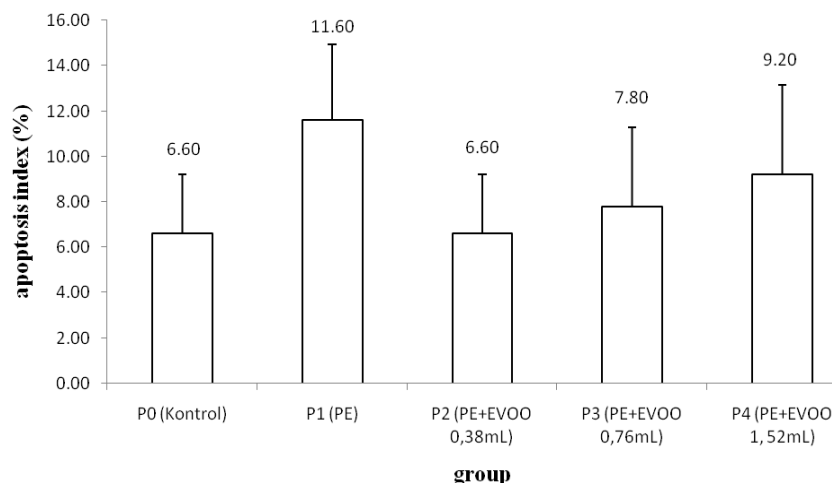


Fig. 2: The effect of EVOO on apoptosis of the placenta index of control and treatment groups.

DISCUSSION

Bcl-2 expression indicated significant difference in Bcl-2 protein expression in the normal group and preeclampsia. In Preeclampsia, there is decreased expression of Bcl-2 protein [8, 15]. Other researchers also reported that, in Preeclampsia, there was a decreased expression of Bcl-2 protein in placental cell syncytiotrophoblasts, resulting in delayed fetal growth. This is due to the failure of spiral artery remodeling that induces free radicals in the mitochondrial membranes of the placental cells, resulting in a decrease in the expression of Bcl-2 protein leading to apoptosis [7]. The expression of the Bcl-2 and Bcl-xl genes is lower in severe preeclampsia pregnancies than in normotensive pregnancies [9].

We suspect the α -tocopherol content in EVOO may suppress p53 activation. It is known that the increase in Bcl-2 expression is thought to be due to p53 inactivation, thus preventing cytochrome c release with Apaf1 and ATP to cause apoptosome not to occur. This causes caspase 9 not to be activated, resulting in apoptotic resistance [16, 17]. Other studies have shown the administration of α -tocopherol ointment on the back of mice after exposure to UV radiation can reduce 55% of the formation of cyclobutane pyrimidine p53 gene dimer that plays a role in the pathogenesis of squamous cell carcinoma [18]. In addition, other researchers stated the combination of vitamin E and exercise was able to suppress free radicals that can damage the DNA production of the p53 gene, so over expression can be suppressed in rat prostate gland tumors [19].

The results of observation on placental cells and the calculation of index apoptosis in this study are not different. Another study shows, in preeclampsia, apoptosis index is higher than the normal pregnancy¹⁵. Meanwhile apoptosis of placenta index of preeclampsia was higher than normal pregnancy, also causing complication of low birth weight of fetus about 14,3% [8].

The process of apoptosis in a normal pregnancy plays a role in the replacement of the cytotrophoblast and renewal of the syncytium surface from the corral villi. The process of apoptosis occurs in syncytiotrophoblast and the cytotrophoblast. This process of increase occurs as the age of pregnancy increases because of decreased expression of Bcl-2 protein that inhibits apoptosis. Therefore, if high levels of Bcl-2 protein expression in syncytiotrophoblast prevent apoptosis in trophoblastic [8], it is suspected the apoptosis index does not differ between groups because apoptotic cell count is performed at the end of pregnancy of rat.

Apoptosis in physiological conditions serves to regulate cell numbers, proliferation, and eliminate cells that are no longer useful as a normal development of cells, such as in embryogenesis, hormone-dependent involution in the menstrual cycle and follicular atresia in menopause, cell deletion in epithelial cell proliferation, excessive reactive cell lymphocyte elimination, cell death induced by cytotoxic T cells in viral infection and tumor progression [20]. Apoptosis is an important process in both normal tissue development and tissue homeostasis in adults, including immune system regulation, for example in T cell lymphocytes, which are cellular immune systems responsible for destroying damaged or infected cells in the body. T lymphocytes undergo maturation in the thymus gland, but before entering the bloodstream, it will be tested to ensure the cell is effective against reaction to normal cells. If there are ineffective or self-reactive T lymphocytes, they will be excluded by apoptosis [21].

However, in pre-eclampsia, immunologic adaptation fails, so the conception persists, but the trophoblast cells are unable to invade the spiral artery to dilate, so the blood vessel tone remains high and

vasoconstriction occurs. This condition causes maternal blood vessels to be unable to produce adequate of blood circulation, so that ischemia will occur and stimulate the occurrence of apoptosis placenta⁸. However, apoptosis is not only due to ischemic placenta, but hypoxia can also be the trigger of apoptosis through the mechanism of cytokines, such as TNF α or Fas ligand, which will activate caspase 8 and caspase 9 as initiators of apoptosis. Caspase 3 and caspase 6 are executors. It is known that free radicals often play a role in the occurrence of preeclampsia but does not entirely cause an increase in apoptosis[22]

We suspect the increase in apoptosis is strong in the P1 group because of the involvement of oxidation reactions that occur due to preeclampsia. This is evidenced by the results of plasma MDA levels at the end of pregnancy in the P1 group, which is higher than other groups. MDA is the end product of lipid peroxide, a free radical. These free radicals will attack cell growth, including DNA, unsaturated fatty acids (PUFAs). When free radicals react with PUFA in mitochondrial cell membrane, the structure and function become damaged. The researchers' allegations are consistent with the opinion that mitochondria play a role in regulating apoptotic processes in preeclampsia [15]. Apoptosis may occur in trophoblast cells involving mitochondria via one of the apoptotic pathways (CD95) or Fas receptor (incorporated in TNF Receptor family) and Fas ligand, referred to as TRAIL (TNF Receptor Apoptosis Inducing Ligand) apoptosis and is called the Extrinsic pathway or the Death Receptor Pathway, but this is not part of the Mitochondrial pathway[15].

Different opinions describe that apoptosis in PE occurs as a result of increased expression of Bax (Bcl-2 family) proteins in intracellular trophoblast cells, which is a proapoptosis protein that interacts with Bcl-xl or binds directly to the outer membrane of the mitochondria, resulting in cytochrome-c release, which will coincide with Apaf-1, procaspase-9, and ATP form the apoptosome, which will activate the path of internal apoptosis [20]. It is known that Bax activated by Bid causes Permeability Transition Pore (PTP) in the outer membrane of mitochondria to become open so that cytochrome-c exits (leaks) resulting in apoptosis. Proteins (Bcl-2 and Bcl-xl) prevent this PTP from occurring, suggesting increased expression of Bax proteins in apoptosis due to preeclampsia provides evidence of mitochondrial involvement in apoptosis¹⁵. Another opinion [15] is that Bax protein activation only does not induce apoptosis, but in this case, p53 also plays a major role in heavy preeclampsia in some trophoblast cells, so the apoptosis index is higher than that of normal pregnancy. However, in this study, there is no known expression of p53 and Bax, so the expression of proteins that play a role in inducing apoptosis is not clearly known [15].

In addition, α tocopherol in EVOO is significantly capable of inhibiting MGO (methyl glyoxal), whose reaction is very high in glucose metabolism and has been known to cause damage and induce apoptosis in endothelial cells. This inhibition of MGO is able to change the production of ROS in intracellular, resulting in increased expression of Bcl-2 protein and decreased Bax protein expression, which can prevent cell apoptosis from widening [23]. This is evidenced in [Fig. 3] above that there is a strong relationship between Bcl-2 protein expression and apoptosis. In addition, α tocopherol in EVOO can attack lipid peroxide, resulting from the reaction between lipids and free radicals in mitochondrial cell membranes that will protect and prevent further damage to the placental endothelial cells.

CONCLUSION

Administration of EVOO may increase Bcl-2 expression in the preeclampsia model. In addition, the apoptotic index of white rat in the preeclampsia model group was in grade III (++) , stronger / higher when compared with treatment group not given EVOO. It is recommended to examine the expression of p53 or Bax protein to find out which protein regulates apoptosis.

CONFLICT OF INTEREST

No conflict of interest

ACKNOWLEDGEMENTS

We would like to convey special acknowledgement to Prof. Dr. Ramlan Silaban, M.Si, University of Medan, North of Sumatera and Dr. Suci Rahayu, M.Si, University of North Sumatera, Medan for their guidance alongside the research

FINANCIAL DISCLOSURE

Self-funded

REFERENCES

- [1] Kemenkes RI. [2013] Profil Kesehatan Indonesia 2012. Pusat Data dan Informasi Kemenkes RI, Jakarta.
- [2] Robert JM, Judith L, Lisa MB, Jose MB, Eduardo B, Anibal M. [2003] Nutrient Involvement in Preeclampsia. *The Journal of Nutrition*. 133:1684-1692.
- [3] Yusniar. [2004] Faktor Risiko Kejadian Preeklampsia dan Eklampsia di RSUD Labuan Baji Makassar. Skripsi. Universitas Hasanuddin, Makassar.
- [4] Matsubara K, Higaki T, Yuko M, Akihiro N. [2015] Nitric Oxide and Reactive Oxygen Species in the Pathogenesis of Preeclampsia. *Int J Mol Sci*. 16: 4601- 4614.
- [5] Chen bao D, Wang W. [2013] Human placental microRNAs and preeclampsia. Mini review. BOR Papers in Press. Vol.10.
- [6] Chio CC, Lin JW, Cheng HA, et al. [2013] MicroRNA-210 targets antiapoptotic Bcl-2 expression and mediates

- hypoxia-induced apoptosis of neuroblastoma cells. Archives of Toxicology. 87:458-468.
- [7] Ishihara N, Matsno H, Murakoshi H, Fernandez JB, Sannoto T, Maruo T. [2002] Increased apoptosis in syncytiotrophoblast in human term placenta complicated by either preeclampsia or intrauterine growth retardation. Am J Obstet Gynecol. 186:158-166.
- [8] Teguh M, C Johannes Mose, Jusuf SE, Betty SH. [2010] Perbedaan indeks apoptosis plasenta antara preeklampsia dan kehamilan normal serta hubungannya dengan berat badan lahir dan tekanan darah ibu, Majalah Kedokteran Bandung, 42(1): 1-5.
- [9] Arianto B, Rumekti HD, Detty SN. [2015] Perbandingan rerata ekspresi Bcl-2 dan Bcl-xl pada preeklampsia berat dan kehamilan normotensi. IPAKESPRO, 2:122-126.
- [10] Takiuti NH, Kahhale S, Zugaib M. Stress in pregnancy: a new wistar rat model for human preeclampsia. Am J Obstet Gynecol. 3: 544-550
- [11] Nakbi A, Tayeb W, Abir G, et.al. [2010] Effects of olive oil and its fractions on oxidative stress and the livers fatty acid composition in 2,4 Dichlorophenoxyacetic acid-treated rats. BioMed Central. 7: 1-11.
- [12] Lopez MJ0, Berna G, Everado MC, Hermina LG, Franz M M Carmen L.[2008] An extra-virgin olive oil rich in polyphenolic compounds has antioxidant effects in Of1 Mice. The Journal of Nutrition, 138:1074-1078.
- [13] Kusumawati D. [2004] Bersahabat Dengan Hewan Coba (:8-50). Gadjah University Press, Yogyakarta.
- [14] Kokawa K, Shikone T, Otani T, et al.[2001] Apoptosis and the expression of Bax and Bcl-2 In hyperplasia and adenocarcinoma of the uterine endometrium. Hum Reprod 16:2211-2218
- [15] Keman K, Prasetyorini N, Langgar MJ. [2015] Perbandingan eskpresi p53, Bcl-2 dan indeks apoptosis trofoblas pada preeklampsia/eclampsia dan kehamilan normal. Maj Obstet Ginekol Indones, 33:151-159.
- [16] Kirkin S, Joos M, Zornig. [2004] The role of Bcl-2 family members in tumorigenesis. Biochim Biophys Act. 1644: 229-249.
- [17] Skommer JT, Brittain S, Rayhaudhuri. [2010] Bcl-2 inhibits apoptosis by increasing the time-to-death and intrinsic cell -to-cell bariations in the mitochondrial pathway of cell death. Apoptosis. 15:1223-1233.
- [18] Weixing Chen, Margaret B, Jessie M, David A and Helen L Gensler. [2009] Inhibitions of cyclobutane pyrimidine dimer formation in epidermal P53 gene of UV- irradiated mice by α tocopherol. Journal nutrition of cancer. 29(3): 205-211.
- [19] Dashtiyani Amin A, Sepehrimanesh M, Nader T, Mohammad EA. [2017] The effect of endurance training with and without vitamin E on expression of p53 and PTEN tumor supressing genes in prostate glands of male rats. Biochimic open. 4 : 112-118.
- [20] Sujatmiko T, Rumekti H Diah, Betty SN. [2015] Perbandingan rerata ekspresi protein Bax dan Bak pada preeklampsia berat dan kehamilan normotensi, jurnal kesehatan reproduksi (IPAKESPRO), Vol:2.3.
- [21] Hermawan AG. [2012] Mekanisme apoptosis pada sepsis. Majalah Kedokteran Terapi Intensif. 02 : 26-32
- [22] Levy R. [2005] The role of apoptosis in preeklampsia. IMAJ. 7:178-181.
- [23] Moon ho Do, Su nam Kim, Seung-Yong Seo, Eui-Ju Yeo, Sun Yeou Kim. [2015] δ - Tochoferol prevents methylglyoxal-induced apoptosis by reducing ROS generation and inhibiting apoptotic signaling cascades in human umbilical vein endothelial cells, Food Funct. 6:1568-1577.

REVIEW

PINEAPPLE [*ANANAS COMOSUS* (L.)] PRODUCT
PROCESSING TECHNIQUES AND PACKAGING: A REVIEW

Tanmay Sarkar, Pritha Nayak, Runu Chakraborty*

Dept. of Food Technology and Biochemical Engineering, Jadavpur University, Kolkata, INDIA



ABSTRACT

Pineapple is one of the most relished fruits in India. In the present literature review, several pineapple varieties like Cayenne, Queen, Spanish, Abacaxi, Kew and Mauritius have been enlisted as well as some pineapple based products like canned pineapple, candied pineapple, pineapple fruit cake, dehydrofrozen pineapple and some other healthy pineapple products have been documented. The processing techniques like canning, baking, osmotic dehydration, freezing, extrusion of fruits etc. for the said products have also been discussed together while describing the products. Some modern packaging techniques have also been discussed to keep the pineapple products available round the year. Some of the products that has been commercialized and ought to be commercialized has been drawn attention in this literature review as pineapple is very important in terms of medicinal values.

INTRODUCTION

Pineapple (*Ananas comosus* L.) is one of the most important commercial fruit crops with several health benefits [1]. It belongs to Bromeliaceae (a large family of American tropics) and is originated from South America [2, 3]. Due to its excellent flavour and taste, pineapple is known as the queen of fruits [1]. The fresh pineapple fruit contains 60% edible portion and the moisture content ranges from 80-85%. The fruit contains 12-15% sugars, 0.6% acid, 0.4% protein, 0.5% ash (mainly K), 0.1% fat, fibre, vitamin A, C and β -carotene and antioxidants mainly flavonoids, citric and ascorbic acid [2,3,4]. The mature fruit contains a proteolytic digestive enzyme [4], Bromelin, which when taken with meals proves to aid in digesting protein by breaking proteins to amino acids. The fruit can be consumed fresh or may be processed into squash, syrup, jelly, vinegar, citric acid to name a few [5,6].

Brazil, Thailand, Philippines, Costa Rica, China and India are major pineapple producing countries and the total area under pineapple cultivation in the world is 909.84 thousand ha with production around 19412.91 thousand tons [1,7]. India has 7% of share in pineapple production across the globe. It is mostly grown in North East region, West Bengal, Kerala, Karnataka, Bihar, Goa and Maharashtra states in India. Pineapple fruit production has increased from 1,362.00 thousand tons in 2006-07 to 1,415.00 thousand tons in 2010-11. West Bengal is the highest in terms of production followed by Assam and Karnataka producing 21.5, 15.6 and 13.1% respectively [7].

Anti-hyperglycemic and analgesic in nature, which leads the way of getting cheaper and alternative option of medicine for reducing blood sugar level in diabetic patients [1,8].

Considering an annual world production of pineapple around 19 million tons [5], only roughly 1/3 is being industrially processed, mainly by canning (30%), juice (4%) and 2/3 is consumed as fresh fruit. To further promote pineapple for industrial processing and value addition, several factors are to be noted: integration of grower and processing industry, fruit type and their application, product portfolio, processing technology, logistics, marketing and promotion, and long term planning [9].

In this review, we seek to document the pineapple cultivars, several products from pineapple and their processing technologies as well as packaging of pineapple.

PINEAPPLE VARIETIES

There are many pineapple varieties which can be divided into four groups namely Cayenne, Queen, Spanish and Abacaxi. There are other cultivars also present like Kew or Giant Kew, Mauritius to name a few [3, 7].

Cayenne

This is the most commonly grown variety of pineapple with high fruit quality. It provides high production, resistance to gummosis and contains spineless leaves. The TSS content of flesh ranges from 12-16°B. Among the Cayenne variety, Smooth Cayenne provides the ideal cylindrical shaped fruit for canning. Other members of Cayenne group are Hilo and Baronne de Rothschild. The first one does not produce slips whereas the second one has spiny leaves [3].

KEY WORDS

Pineapple based products,
Modern packaging,
Pineapple varieties

Received: 13 April 2018
Accepted: 22 May 2018
Published: 5 July 2018

*Corresponding Author

Email:
crunu@hotmail.com
Tel.: +91-9831122626

Queen

The leaves of the fruit are short having many spines which curve back. The fruit yield is moderate and the shape is conical, therefore unsuitable for canning. The flesh of the fruit is golden yellow in colour with outstanding aroma. The eyes of the fruit are small and raised. The TSS content of the flesh ranges from 15-16°B. Natal Queen, Z Queen, Ripley Queen are the subgroups present in this cultivar. The plants of this variety are resistant to most diseases [3].

Spanish

This cultivar has long, narrow, spiny leaves with few, but large, flat eyes. This round shaped variety is pretty good for fresh fruit export but moderate for canning purposes. The flesh is fibrous, deep golden yellow in colour and the TSS ranges between 10-12°B. Singapore Spanish has got smooth leaves and is also good for canning [3].

Abacaxi

Among the Abacaxi group, Pernambuco variety has long spiny leaves and a very long fruit stalk. This pyramid shaped locally consumed fruit has white flesh colour. This variety produces many slips and unsuitable for canning or exporting as fresh fruit [3].

Kew or Giant Kew

Fruits of this cultivar are big in size and deep yellow to coppery yellow in colour. The colour of the flesh is pale yellow to yellow and comes with broad, flat eyes. The TSS content of the flesh ranges from 12-14°B [7].

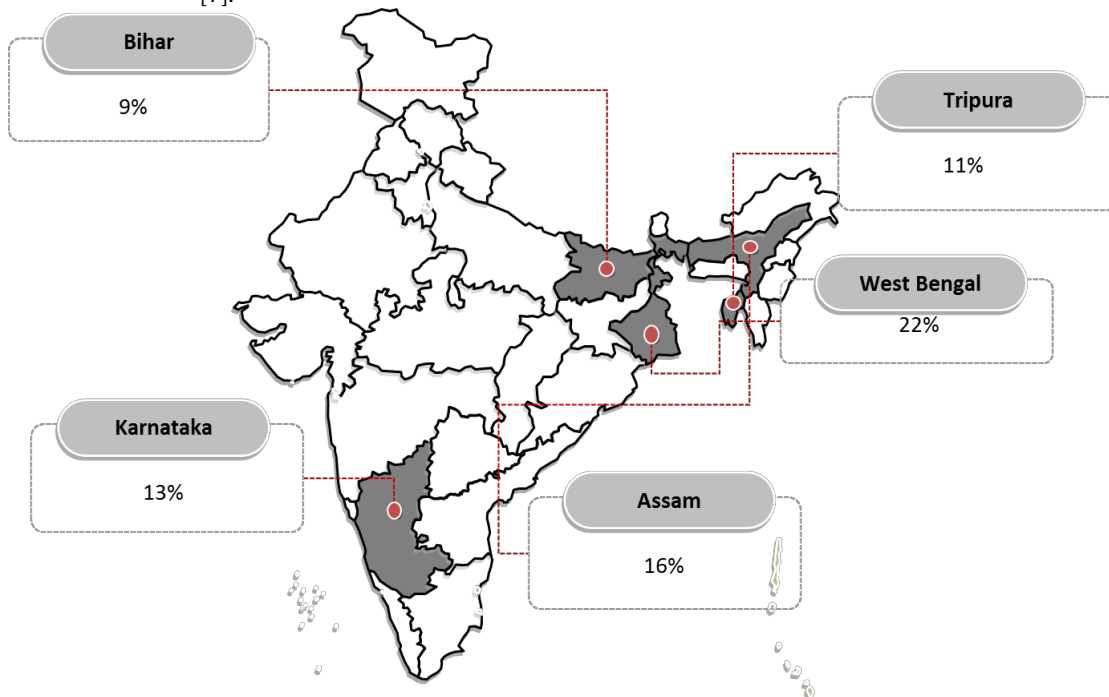


Fig. 1: Leading pineapple producing states in India.

PINEAPPLE PRODUCTS

Canned pineapple

Pineapple is firstly removed from the shell including eyes and cut into cubes of dimension approximately 0.5 cm×0.5 cm×0.5 cm. The cut cubes are blanched for 1 min in hot water at about 90°C and then cooled in tap water [10]. Orange juice, Mango juice and 40% (weight of sucrose/weight of water) sucrose can be used as filling liquor inside the can. Orange and Mango juice TSS content are also adjusted to 40°B. Citric acid and potassium sorbate are added to each solution at 0.2% and 0.1% concentration levels. Pineapple cubes are divided into three parts and each part of pineapple is packed individually with the previously

prepared solutions at a ratio 2:1 of cubes and solution weights. The canned pineapple is generally pasteurized at 90°C for 5 minutes, then cooled and stored at room temperature [11].

Candied pineapple

Pineapples are cleaned, peeled and size reduced into cubes. Then dipped in sucrose solution and food colour is added. Candied pineapple is prepared by boiling until all the syrup was absorbed by the pineapple [4].

Pineapple fruit cake

The batter for the pineapple fruit cake may be prepared by the creaming method. In 500 g of sugar, 1 kg of margarine is mixed using the cake mixer until the batter becomes light and fluffy [12]. In another bowl, eight large eggs are whisked until foamy and firm, then 2 kg of wheat flour and 4 teaspoons baking powder are sieved together with half (1/2) teaspoon of nutmeg. The whisked eggs and flour mixes are folded into the sugar and margarine batter, after that the candied pineapple are added into the cake mix and loaded into a greased pan and baked in an oven at 150°C for 1h [4]. The pineapple cake contains 9.34% protein, 30.97% moisture, 46.97% fat, 0.23mg/100g magnesium, 97.53mg/100g calcium which implies this product is a good source of trace elements that is important to the body as enzyme co-factors and acts as building blocks respectively.

Dehydrofrozen pineapple

The osmotic dehydration is carried out using a sucrose hypertonic solution of 60°B at 40°C. Osmotic dehydration is carried out in a shaker, with a frequency of 75 horizontal oscillations per min, and 1 cm amplitude, containing a 6 Erlenmeyer flask rack. Pineapple samples are placed into each Erlenmeyer that contains 500 ml sucrose solution at 40°C. At pre-established times (30, 60, 120, 180 and 240 min) one Erlenmeyer is removed, and each sample is rinsed with demineralized water at 8°C for 3–5 seconds in order to remove the remaining syrup, and the excess of water is eliminated too, blotted with tissue paper. Afterwards, one portion of this processed fruit is frozen. Osmotic dehydration assays at 45°C are carried out and a fraction is frozen for 12 h. Then it is kept at constant temperature (20°C) in a capped flask for 2 h (for thawing).

Drying is performed in a transversal flow dryer under constant conditions of air velocity (1.5m/s) and temperature (45, 60 or 75°C). Slices of pineapple are placed in aluminum baskets, avoiding any contact among fruit pieces. Samples are extracted from basket and frozen.

Samples of partially dehydrated pineapples are restored at 4°C in capped plastic containers for 12 h prior to freezing. Then, these samples are placed on perforated stainless steel trays, and frozen in chambers with air circulation at $-31.5 \pm 2^\circ\text{C}$. During this process copper-constantan thermocouples connected to a data acquisition device are placed in the center of sample which has been processed by different periods of osmotic dehydration; one thermocouple is placed inside the freezer chamber. After 2 h, samples are removed from the chamber, and the thawing process is carried out at constant temperature (20°C) for 2 h, in capped flasks [13].

Pineapple juice

Pineapple juice comes from various places in the processing line of pineapple. It is generally obtained by pressing the shell (cut or scrapings) in the Ginaca machine. It peels the pineapple and forms cylinders from which the slices are made. The small fruits may be chosen which are unsuitable for canning and the fruit portions from drainage crushed pineapple operation. The solid material is then shredded and filter aid (infusorial earth) is mixed with the shredded pieces of pineapple followed by pressing in a hydraulic press. Then the liquid material is subjected to heating to coagulate solids to form thin slurry which then passed through a continuous centrifuge. This removes all the suspended solids including the fibers and other coarse small particles. Pineapple juice is sometimes homogenized to get a cloud stable juice [14]. Pineapple juice is used to treat any type of morning sickness, motion sickness or nausea. Roasted pineapple juice has been utilized for treatment of strangury by different communities in Assam, India [15]. Juice of pineapple is also beneficial for fevers and cystitis [16].

Crushed pineapple

To prepare crushed pineapple, shredded pineapple is first pumped into steam jacketed kettles and heated to 90°C. To ensure optimum consistency of the product some of the juice is drained away. Sufficient heavy sucrose syrup (23°-35°B) is added to the product if it is to be sweetened. The hot mixture is automatically packed into cans, sealed after giving a short heat processing to ensure quality and finally cooled [14].

Pineapple concentrate

Pineapple juice may be concentrated in multiple effect vacuum pans or the vacuum pans which operate at below 60°C. If short time evaporators are used, high temperatures up to 82°C have been used successfully. Fresh pineapple juice (12°B) is concentrated up to 45°B for retailing or may be concentrated as high as 60°-65°B for reusing in other pineapple based manufacturing processes. Recovered essence is mixed with the concentrate and then it is slush frozen and packed either into metal containers (for 45°B) or polyethylene (PE) lined fiberboard containers (for 65°B). Freezing occurs at -23°C. Bulk pineapple concentrate is also added to citrus juices to form frozen juice blends. Pineapple concentrate is also used to produce many types of canned fruit drinks like canned pineapple-grapefruit drink. This drink has exceeded the volume of production of single strength pineapple juice [14].

Frozen pineapple

Rectangular chunks of pineapple are used to prepare frozen pineapple. The slices can be kept well in syrup of 25°-49°B for 1 year but forms a stale taste. Ascorbic acid may be added to stabilize the flavor in this case. Smooth Cayenne variety is mainly used for freezing application. The Red Spanish variety develops off-flavors if frozen. Pineapple, due to its fiber content, maintains a good texture after thawing. Pineapple for freezing application is prepared in almost the same manner as in canning, except that the cylinders are passed through additional coring operation to remove the last vestiges of fibrous core. Fruits in bins arrive from the plantation are unloaded onto conveyor belts or into flumes of water and washed thoroughly. After grading into 3-4 sizes, they are peeled and cored in the Ginaca machine. Cored cylinders are inspected, trimmed and diverted to another coring machine followed by fixed blade chunk cutter. Chunks are then filled into 211mm×414mm or No. 10 cans followed by addition of syrup, seaming and conveying directly onto air blast tunnel freezer at -34°C. The bulk frozen packages are directly filled from the product line in form of tidbits. Then syrup is added and frozen in a low temperature blast freezer [14].

Pineapple granules

These are made up of 88% soluble solids, mainly sugars, 10% insoluble solids and 2% moisture. They are yellow in colour and passes through a No. 10 mesh screen. Analysis of reconstituted granules show that it have titratable acidity of 0.6, pH 3.7 and TSS 15°B. Granules are generally packed in controlled humidity with a PE bag inside a fiberboard box. Granules are used as a fruit extender, flavor and colour carrier, decorative material and as fruit solids in sauce preparations in bakery goods, dry mixes, cereals, candies, ice cream, gelatin. The low pineapple flavor of granules is increased by using cloudless pineapple juice concentrate (72°B) and reconstituted by mixing 1 part concentrate to 5.5 parts water [14].

Yogurt fortified with pineapple peel powder (PPP)

Crushed pineapple peel is immersed for 30 min in hot water (90°C) to inactivate the proteolytic enzymes and potential pathogens and then it is freeze dried to produce a fine powder. The particle size of powder is standardized to less than 180 μm using sieves followed by sterilizing in UV irradiation for 30 minutes. Set-type yogurts are prepared as described in [17]. Briefly, three lots of milk bases are prepared by reconstituting skim milk powder in warm pure water at 14% (w/v); two lots are then further fortified separately with 1% (w/v) inulin or PPP. Control (without prebiotic supplementation), inulin and PPP fortified milk bases are homogenized and heated to 85°C for 30 min, then cooled to 45°C and aseptically inoculated with 1% (v/v) of each *S. thermophilus* and *L. bulgaricus* cultures. These samples are then divided into two equal portions; one portion is further inoculated with 1% (v/v) of each of *L. acidophilus*, *L. casei* and *L. paracasei* cultures. The final mixes are poured into polystyrene (PS) cups. Then the mixes are incubated at 42°C in an incubator until pH of 4.5 ± 0.05 is achieved. The yogurts are then immediately cooled and stored at 4°C [18].

Pineapple leather

Pineapple is washed, peeled and cut into small pieces followed by grinding in a mechanical grinder to obtain uniform pulp. The extrusion cooking can be carried out in single screw extruder (vented extruder with L/D ratio 30:1 and 22 mm×3 mm die opening). Pineapple fruit pulp can be extruded at lower temperature and screw speed to prevent the phytochemical losses during extrusion cooking. The extrusion cooking is carried out at a barrel temperature of 60-100°C with a screw speed of 50 to 150 rpm. The TSS content of the sample is measured using refractometer in term of brix. Keeping starch (thickening agent) content constant at 2% level, it is added to the fruit pulp and the TSS of pulp is maintained from 10-20°B using sugar. Pineapple fruit leather is dried at 60°C for 1h after extrusion to maintain 20% moisture content in final product. Around 1g of fruit leather is taken and extracted in 20 mL of the solution (16:4 v/v, methanol: water). The extract is then placed in an incubator shaker at 30°C for 5 h followed by centrifugation at 10,000 rpm for 10 min. After centrifugation, the supernatants are stored at -4°C for further analysis like phytochemical properties. Extrusion cooking of fresh produce can be used to enhance the antioxidant activity of the product during processing but it affects most of the phytochemical compounds adversely with the change of temperature, screw speed and brix. The antioxidant activity of pineapple fruit leather increases with increasing barrel temperature [19].

Table 1: Some pineapple based products and their processing techniques

Name of Products	Technology Used	Reference
Canned pineapple	Canning	14, 15
Candied pineapple cake	Creaming, Baking	4
Dehydrofrozen pineapple	Osmotic dehydration, freezing	17
Pineapple juice	Pressing in hydraulic press	1
Pineapple concentrate	Multiple effect vacuum pans	18
Frozen pineapple	Freezing	18
Pineapple leather	Extrusion	23

PINEAPPLE PACKAGING

Edible coating

High molecular weight chitosan (CH), with a deacetylation degree of 82.7%, in 1 wt% acetic acid solution, 98% glacial acetic acid, 1 N sodium hydroxide (NaOH), oleic acid (OA), Tween 80 and food-grade methyl cellulose (MC) have been used to obtain the film-forming dispersions of chitosan. The mixtures are emulsified at room temperature using a rotor-stator homogenizer at 13,500 rpm for 4 min and the pH of all film-forming emulsions is adjusted to 5.2 with 1 N NaOH.

Sodium caseinate (NaCas), calcium caseinate (CaCas), beeswax (BW), oleic acid (OA) and glycerol can be used to obtain the film-forming emulsion of caseinate. Pure sodium caseinate and a mixture of NaCas:CaCas (1:0.5 mass ratio) are dispersed in distilled water. The protein: glycerol ratio is set to 1:0.3 and the protein: lipid ratio is set to 1:0.5 in the emulsions. The lipid part is composed of OA: BW (70:30 mass ratios). After addition of glycerol to aqueous solutions of caseinates, all dispersions are heated to 85°C and the amount of beeswax required is added, which melts in the hot solution. After that, it is homogenized at 85°C for 1 min at 13,500 rpm, then for 1 min at 20,500 rpm. The emulsions are then cooled at room temperature and oleic acid is added. Each emulsion is homogenized again with a vacuum high-shear probe mixer for 2 min at 20,500 rpm and finally they are degasified at 7 mbar at room temperature with a vacuum pump.

Four application techniques have been used for coating cylindrically cut pineapple samples. Method I consists sample drying until $a_w = 0.75$ and afterwards dipping at atmospheric pressure in the film-forming solutions for 5 min, with subsequent coating and drying at room temperature; method II consists of sample dipping at atmospheric pressure in the film forming solutions for 5 min before drying until $a_w = 0.75$; in method III sample is dipped at atmospheric pressure in the film-forming solutions two times (each time 5 min), before drying until $a_w = 0.75$; and method IV consists sample dipping in the film-forming solutions applying a vacuum impregnation operation before drying until $a_w = 0.75$. The vacuum impregnation operation consists of applying a vacuum pulse (50 mbar for 3 min) to the immersed sample, and then restoring the atmospheric pressure while the sample remains immersed for 2 min more. In all the cases, the said procedure is carried out at 25°C and the ratio of the weight of coating solution: sample is 20:1 [20].

UV-C light treatment and packaging into PA/PE pouches

Samples are prepared by removing crown leaves and fruit bottom and then the pineapples were peeled, cored and wedged using a pull-down manual equipment. Pineapple stick is obtained and one stick is introduced to UV-C light treatment (200 J/m²) and packed into PA/PE pouches (30×15 cm, 0.090 mm, 20/70), which are then sealed [14].

Packaging into PA/PE pouches and UV-C light treatment

Samples are prepared by introducing one untreated pineapple stick into a PA/PE pouch followed by sealing the pack and UV-C light treatment (200 J/m²). The irradiance on the pineapple stick surface has been found to be 32 W/m², due to the 20% screening effect of the plastic material. These samples are then exposed to 160 J/m² UV-C light fluence.

UV-C light treatments have shown to exert a high potential for shelf life extension by decreasing microbial growth during storage. The treatment is also efficacious even when the product is packed before exposure to light, which potentially allows in preventing post-treatment contaminations during processing. However, there is a limitation that this process requires packaging single fruit sticks to avoid shadowing effects among food items. In addition, it is mandatory to adopt unprinted packaging materials which allow transmittance of UV-C light and therefore, there is a need for consideration of applying label or a secondary printable package to provide the consumer with the necessary information [21].

Packaging using bio preservative on fresh cut pineapple

Nisin possesses a broader antimicrobial activity than most other bacteriocins and has been shown to be of no or low toxicity. It also has successful functions as a food preservative. The inhibitory effect of nisin is wider than most bacteriocins and it extends to a large variety of gram positive bacteria including spore formers [22]. Solubility of Nisin is good in low pH (3-4) condition. Nisin solution (pH 3-4) is prepared by dissolving citric acid solution in different concentrations of 0.04, 0.05 and 0.06mg followed by soaking them in the above solutions for 5 to 10 minutes. Then it is surface dried for one hour, packed in Polystyrene container and the samples are stored at room (around 25°C) and refrigeration temperature (4°C) for its storage stability.

The bacterial population gets decreased during the storage period for samples treated with bio preservatives compared to control samples with no nisin. Ascorbic acid content in fresh cut pineapple treated with nisin packed in polypropylene is 25.82% at room temperature with a shelf life of 3 days and 28.90% in refrigerated condition with the shelf life of 12 days. The initial total antioxidant activity has been checked as 19.00µg/g in control. In the case of fresh cut pineapple treated with nisin, the total antioxidant activity ranged from 12.30 to 16.00µg/g when stored in differed packaging material at room and refrigerated temperature and checked after 3 days and 12 days of storage respectively [23,24].

CONCLUSION

Pineapple is one of the most relished fruits with ample amount of bioactive compounds present in it. The world pineapple demand has been increasing rapidly. Therefore pineapple and pineapple based products will be of a great demand in recent future not only because of its taste but also a principal compound in terms of health healing in different manner. It is a common fruit in India as well as in some other countries of the world and it contains good amount of various vitamins, carbohydrates, crude fibre, water, different minerals. Generally, the matured pineapple fruit is consumed fresh and juice as source of many essential minerals and vitamins but can also be processed to produce different pineapple based products. Fresh pineapples are rich in bromelain which is used as anti-inflammatory agent as well as reduces swelling in inflammatory conditions such as acute sinusitis, sore throat, arthritis, gout. The Honey Queen Variety of Bangladesh is superior in nutritional content as well as sweetness than the Giant Kew variety of pineapple. Farmers spray growth boosting chemicals and hormones on pineapple flowers to produce large fruit and also apply hormones for early harvesting which may increase the risk of contamination of food materials. Unripe pineapple in some cases is inedible, poisonous and irritates the throat and acts as a purgative. Excessive consumption of ripe pineapple cores leads to formation of fibre balls in the digestive tract. So, beside its high nutritional value there may have some side effects if not consumed properly. To get the fruit and fruit based products available round the year, there should be proper packaging of the processed fruits also. Several conventional techniques like canning and some modern techniques like edible coating, UV ray application, packing by bio preservatives are to be used commercially. There has to be more new products developed from pineapple with keeping or enhancing the nutritional value by modern packaging techniques to provide health benefits to the consumers.

CONFLICT OF INTEREST

There has been no conflict of interest in relation to the work.

ACKNOWLEDGEMENTS

None

FINANCIAL DISCLOSURE

None

REFERENCES

- [1] Hossain MF, Shaheen A, Anwar M. [2015] Nutritional Value and Medicinal Benefits of Pineapple. *International Journal of Nutrition and Food Sciences*. 4(1): 84-88.
- [2] Silva DIS, Nogueira GDR, Duzzioni AG, Barrozo MAS. [2013] Changes of antioxidant constituents in pineapple (*Ananas comosus*) residue during drying process. *Industrial Crops and Products*. 50: 557-562.
- [3] Samson JA. [1980] *Tropical Fruits*. Longman Group Limited, London.
- [4] Offia Olua BI, Edide RO. [2013] Chemical, Microbial and Sensory Properties of Candied-Pineapple and Cherry Cakes. *Nigerian Food Journal*. 31(1): 33-39.
- [5] FAO. [2004] *Food and Agriculture Organization of United Nations*.
- [6] FAO. [2005] *Food and Agriculture Organization of United Nations*.
- [7] *Indian Horticulture Database* [2011].
- [8] Ramachandran A, Ma RCW, Snehalatha C. [2010] Diabetes in Asia. *Lancet* 375: 408-418.
- [9] Riya MP, Antu KA, Vinu T, Chandrakanth KC, Anilkumar KS, Raghu KG. [2013] An invitro study reveals nutraceutical properties of *Ananas comosus* (L.) Merr. Var. Mauritius fruit residue beneficial to diabetes. *J Sci Food Agric*. 94: 943-950.
- [10] Reinhardt A, Rodriguez LV. [2009] Industrial processing of pineapple – trends and perspectives. *Acta Hort*. 822: 323-328.

- [11] Aiboon KL. [2011] Effects of temperature and slice thickness on drying Kinetics of pumpkin slices. *Walailak J. Sci. Tech.* 8 (2):159- 166.
- [12] Assous MTM, Saad EMS, Dyab AS. [2014] Enhancement of quality attributes of canned pumpkin and pineapple. *Annals of Agricultural Science.* 59(1): 9-15.
- [13] Wilton C. [2009]. Cake recipe.
- [14] Ramallo LA, Mascheroni RH. [2010] Dehydrofreezing of pineapple. *Journal of Food Engineering.* 99: 269-275.
- [15] Woodproof JG, Luh BS. [1975] Commercial fruit processing. The AVI publishing company, INC.
- [16] Saikia B. [2006] Ethno medicinal plants from Gohpur of Sonitpur district, Assam. *Indian J. Tradit. Knowl.* 5(4): 529-530.
- [17] Hossain MA, Rahman SMM. [2011] Total phenolics, flavonoids and antioxidant activity of tropical fruit pineapple. *Food Research International.* 44: 672-676.
- [18] Sah BNP, Vasiljevic T, McKechnie S, Donkor ON. [2014]. Effect of probiotics on antioxidant and antimutagenic activities of crude peptide extract from yogurt. *Food Chemistry.* 156: 264-270.
- [19] Sah BNP, Vasiljevic T, McKechnie S, Donkor ON. [2016] Physicochemical, textural and rheological properties of probiotic yogurt fortified with fibre-rich pineapple peel powder during refrigerated storage. *LWT - Food Science and Technology.* 65: 978-986.
- [20] Sharma P, Ramchiary M, Samyor D, Das AB. [2016] Study on the phytochemical properties of pineapple fruit leather processed by extrusion cooking. *LWT - Food Science and Technology.* 72: 53-543.
- [21] Talens P, Pérez-Masía R, Fabra MJ, Vargas A, Chiralt A. [2012] Application of edible coatings to partially dehydrated pineapple for use in fruit-cereal products. *Journal of Food Engineering.* 112: 86-93.
- [22] Manzocco L, Plazzotta S, Maifreni M, Calligaris S, Anese M, Nicoli MC. [2016] Impact of UV-C light on storage quality of fresh-cut pineapple in two different packages. *LWT - Food Science and Technology.* 65: 1138-1143.
- [23] Abee T, Broughton JD. [2003] Bacteriocins-Nisin. *Food preservative.* Springer International Edition, Kluwer Academic / Plenum Publishers, New York, 146-147.
- [24] Sindumathi G, Amutha S, Kavitha V. [2017] Impact of Packaging Materials on Quality of Fresh Cut Pineapple Using Biopreservative to Ensure Safety. *International Journal of Current Microbiology and Applied Sciences.* 6(12): 789-800.

ARTICLE

TEST OF HYPOGLYCAEMIC FUNCTION IN WHITE RAT (*RATTUS NORVEGIUS* W) UPON ADMINISTRATION OF FRACTIONS OF EXTRATS OF AFRICAN LEAF (*VERNONIA AMYGDALINA* DEL)

Lavinur*

Studi program Farmasi, Poltekkes Kemenkes Medan, INDONESIA

ISSN 0976-3104



ABSTRACT

Vernonia amygdalina Del is plant with various functions. It multipurpose attributes and rapidly regenerating soft wooded shrub characteristics makes it very special. Beyond been used in disease treatment, it also is a good source of good nutrients for the body. *V. amygdalina* was the most popular for it antidiabetic characteristics and it was noted that where oral intake of hot water *V. amygdalina* leaves extract (500 mg/kg) was administered, it reduced blood glucose concentration. The present research is an experimental study and it commenced by weighing the rats. The weights of the rats used range from 150-200 g. these rats were made diabetic by continuous administration of glucose. After the diabetic state was achieved, the trial commenced to assess the impact of fractionated concentrate of African leaf on reduction on blood glucose in these rats. From the result of the experiment on the white rats, effect of EEAL on blood glucose wasn't statistically significance ($p > 0.005$) but that of HEAL was significance ($p < 0.005$). This further authenticates the benefit of African leaf in management of diabetes. It therefore can be concluded that it has a hypoglycemic attribute and if used by humans it can help individual easily reduce hyperglycemia.

INTRODUCTION

KEY WORDS

African leaf, hypoglycemia, diabetes mellitus, blood glucose.

Vernonia amygdalina Del is plant with various functions. It multipurpose attributes and rapidly regenerating soft wooded shrub characteristics makes it very special. It is about 2 to 10 m tall with petiolate leaves of around 6 mm in diameter. It is widely spread geographically accounting for the various names it is known as. It is a species under the genus *Vernonia* Shrub (Family: Compositae; Order: Asterales; S/C: Asteridae; Classes: Dicotyledons) which contains about 1000 species. More than 500 of these *Vernonia* plants are distributed in Africa and Asia, approximately 300 in Mexico, Central and South America. When using African as a case study, the African widely grown in the western part of the continent of Africa especially in Nigeria. It has various medicinal attributes and used from ages past. Also it is characteristically a tropical plant making it thrive well irrespective of adverse weather condition or change in climate. In traditional medicine, African leave can be used as an herbal treatment for various kinds of the disease. [1]

Beyond been used in disease treatment, it also is a good source of good nutrients for the body such as phenolic acids, fatty acids, vitamins, essential acids, specially oils, antioxidants, mineral sources and anti-inflammatory agents [2]. The leaf is beneficial because it is involve in making people healthier and this is attributed to its various constituents. Diabetes mellitus is a metabolic disorder resulting from a defect in insulin secretion, insulin action, or both. Insulin deficiency in turn leads to chronic hyperglycemia with disturbances of carbohydrate, fat and protein metabolism [3]. Quite difficult to believe but through that every 17 seconds, someone in the world dies of diabetes related causes. In the same 17 seconds, another two people are diagnosed with the disease for the rest of their life and may suffer increased morbidity and reduced quality of life, premature death, and large adverse economic effects due to higher healthcare and non-healthcare costs [4]. Globally, type 2 diabetes disproportionately affects the working age population; 46% of those affected are aged 40–59 years, and half of all diabetes-related deaths occur in individuals under age 70 [5]. Type 1 diabetes mellitus may present at any age but most typically presents in early life with a peak around time of puberty [6]. Diabetes mellitus is a chronic disease which affects millions of people worldwide and the prevalence of this disease was projected to reach 300 million before year 2025 [7]. *V. amygdalina* was the most popular for it anti-diabetic characteristics in Nigeria [8, 9]. Studies have shown that anti-diabetic potential of *V. amygdalina*. It was noted that where oral intake of hot water *V. amygdalin* leaves extract (500 mg/kg) was administered, it reduced blood glucose concentration of both normoglycaemic and hyperglycemic rats induced by alloxan (10). The aim of this research is to test of hypoglycemic function in white rat (*Rattus norvegius* W) upon administration of fractions of extracts of African leaf (*V. amygdalina* DEL).

MATERIALS AND METHODS

Prior to start of this study an ethical clearance letter has been obtained from the Animal Research Ethics Committee (AREC) of Universitas Sumatera Utara, Medan, Indonesia. The present research is an experimental study and it commenced by weighing the rats. The weights of the rats used range from 150-200 g. these rats were made diabetic by continuous administration of glucose. After the diabetic state was achieved, the trial commenced to assess the impact of fractionated concentrate of African leaf on reduction on blood glucose in these rats. For this study a total of forty-five white male rats (*R. norvegius*) were used and divided into groups

Received: 13 May 2018
Accepted: 14 June 2018
Published: 6 July 2018

*Corresponding Author
Email: lavinur2@gmail.com
Tel: +62-81292722656

of 15 with each group consisting of 3 rats each. The effect of the African leaf was studied by giving the extracts to these rats orally. After this is done, a period of 15 minutes is waiting for before the rodent glucose levels were checked each. Out of the total 15 groups, three groups of the rats served as control. One of the controls was given distilled water; another given CMC suspension with both serving as negative controls and the third group was given suspension of glibenclamide to serve as a positive control. The remaining 12 groups were given the African leaf extracts. A section of the African Leaf extracts was made into suspension using ethanol focus of African leaf (EEAL) and administered at 100, 200 and 300 mg/kg body weight of rats and this had effect on the hyperglycemic state of the rats, another was made into suspension using fractionated n-hexane think of African leaf (HEAL) does not hyperglycemic affect and the last suspension was made using fractionated ethyl acidic corrosive deduction focus of African leaf (EAEAL) at 200 and 300 mg/kg body weight of rat and this also have effect on the hyperglycemic state of the rats. When the test was completed, test of decrease in blood glucose level was done. With help of ANOVA blood glucose level of mice has analyzed and test have identified at 95% confidence level. From the result in this ANOVA test and method it has been identified that there were significant difference and then continued used with Duncan test to determine which group were having important different using SPSS (Version22).

RESULTS AND DISCUSSION

From the result of the experiment on the white rats it has been found that Africa leaf is one of the best plants that can be used as herbal treatment for various diseases and it is useful in control of blood glucose and therefore will be beneficial in the management of diabetes. After the experiment on the 45 rats it has been identified that the rats administered African leaf extracts had a decrease in body weight that is approximately average to their initial weigh before induction of the diabetic state and also their blood glucose level decrease as well by 5%. [Table 1] shows the frequency distribution of body weights of the rats used in this study as well as the minimum and maximum weight respectively. Also the Mean Weight and Standard Deviation is shown in [Table 1]. The effect of EEAL on blood glucose wasn't statistically significance ($p > 0.005$) but that of HEAL was significance ($p < 0.005$) and this are shown in [Table 2] and graphically represented in [Fig. 1] below.

Table 1: Frequency Distribution characteristics of Body Weight of Rats Used

Body Weight of Rats (Grams)	No	Percentage (%)
150 -159	25	55.56
160 -169	17	37.78
170 -179	2	4.44
180 -190	1	2.22
Total	45	100

Maximum weight = 180 Minimum weight = 150 Mean = 158.91 SD = 6.56

Table 2: Results for ANOVA Test of Gilbenclamide, EEAL and HEAL

	N	Mean	Standard Deviation
Gilbenclamide	3	113.33	5.51
EEAL 100 mg/kg	3	117.67	2.08
EEAL 200 mg/kg	3	118.67	3.22
EEAL 300 mg/kg	3	113.00	5.29
Gilbenclamide	3	113.33	5.51
HEAL 100 mg/kg	3	131.33	2.52
HEAL 200 mg/kg	3	127.67	1.53
HEAL 300 mg/kg	3	122.00	2.00

EEAL Value for $p = 0.312$ (Not Statistically Significant)

HEAL Value for $p = 0.001$ (Statistically Significant)

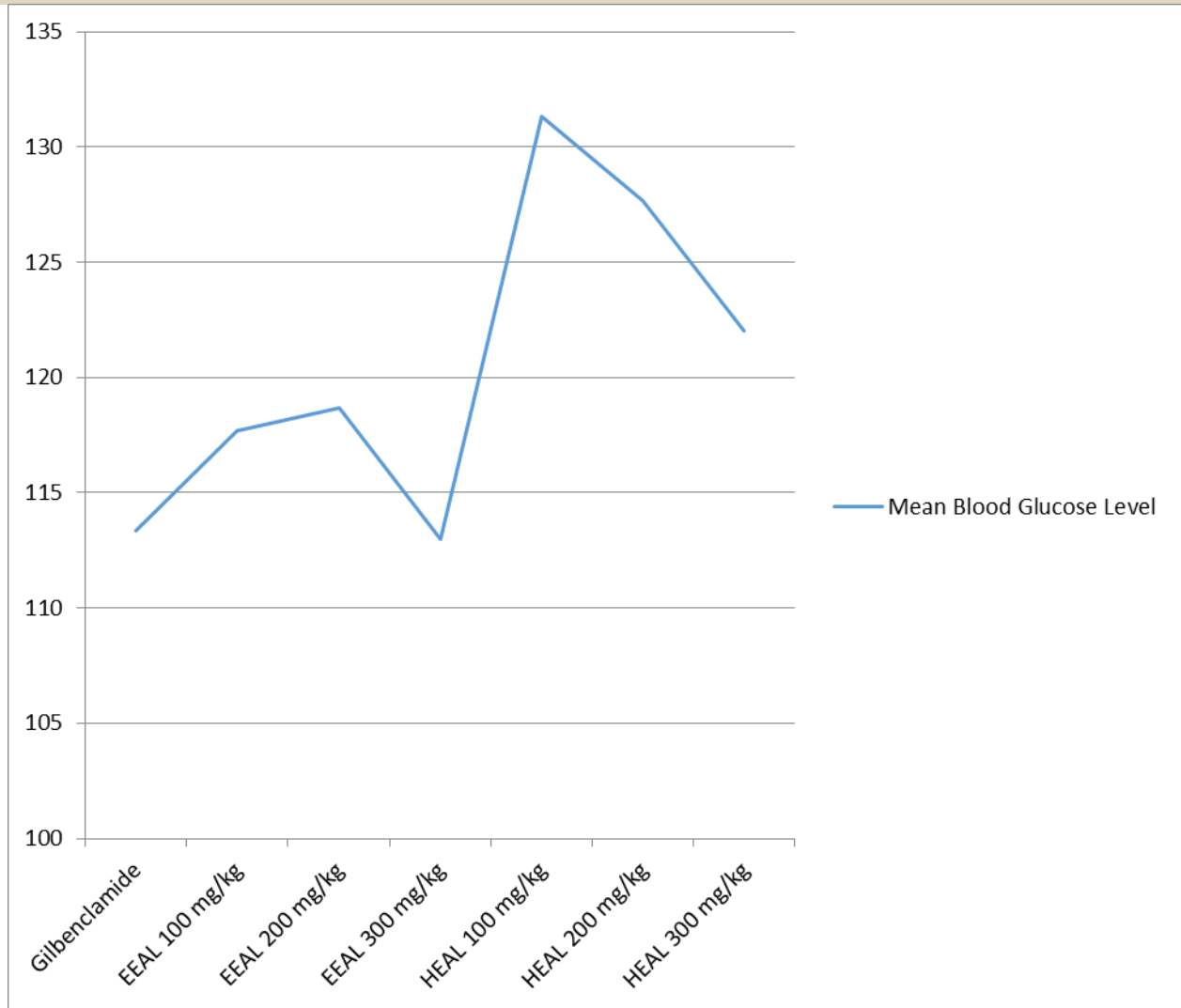


Fig. 1: Graphical Representation showing Changes in Blood Glucose of Rats Given Gilbenclamide, EEAL and HEAL Respectively.

CONCLUSION

The relationship between African leaves and health is indispensable, furthermore it is rich has nutritional value as it constitute of phenolic acids, fatty acids, vitamins, essential acids, oils, antioxidants, mineral sources and anti-inflammatory agents. A significant hypoglycemic activity with weight loss was noticed in the rats when African leaf was used in diabetic management in diabetic rats. Hence it could be concluded that African leaf has hypoglycemic function in patients suffering from hyperglycemia.

CONFLICT OF INTEREST

Nil

ACKNOWLEDGEMENTS

I would like to convey thank head of animal research ethics committee(AREC), fakultas matematika dan ilmu pengetahuan Alam- Universitas Sumatera Utara for kindly lending me the ethical approval letter No. 187/KEPH-FMIPA/2016 to carry out the research.

FINANCIAL DISCLOSURE

Self- funded

REFERENCES

- [1] SweeKeongYeap, Wan Yong Ho, Boon KeeBeh, Woon San Liang, Huynh Ky1, Abdul HadiNoaman Yours1 and NoorjahanBanuAlitheen. *Vernonia amygdalina*, an ethnoveterinary and ethnomedical used green vegetable with multiple bioactivities. *Journal of Medicinal Plants*. 2010; 4(25): 2787-2812.
- [2] Yattoo MI, Saxena A, Gopalakrishnan A, Alagawany M, Dhama K. Promising antidiabetic drugs, medicinal plants and herbs: An update. *International Journal of Pharmacology*. 2017;13:732-745.
- [3] Sena CM, Bento CF, Pereira P, Seiça R.[2010] Diabetes mellitus: New challenges and innovative therapies. *EPMA J*. 1(1): 138-163.

- [4] Efiang E.E, Igile GO, Mgbeje BIA., Ou EA, Ebong PE. [2013] Hepatoprotective and antidiabetic effect of combined extracts of *Moringaoleifera* and *Vernonia amygdalin* in streptozotocin-induced diabetic albino Wistar rats. *J. Diabetes and Endocrinol.* 4(4): 45-50
- [5] Rawal LB, Tapp RJ, Williams ED, Chan C, Yasin S, Oldenburg B. [2012] Prevention of type 2 diabetes and its complications in developing countries: A review. *Int J Behav Med.* 19(2):121-133.
- [6] El-Abhar HS, Schaal MF. [2014] Phytotherapy in diabetes: Review on potential mechanistic perspectives. *World J Diabetes.* 5(2):176-197. DOI: 10.4239/wjd.v5.i2.176.
- [7] Farombi EO, Owoeye O. [2011] Antioxidative and chemopreventive properties of *Vernonia amygdalina* and *Garcinia biflavanoid*. *Int J Environ Res Public Health.* 8:2533-2555.
- [8] Adesanoye OA, Farombi EO. [2010] Hepatoprotective effects of *Vernonia amygdalina* (astereaceae) in rats treated with carbon tetrachloride. *ExpToxicolPathol.* 62:197-206.
- [9] Adiukwu PC, Amon A, Nambatya G, Adzu B, Imanirampa L et al. [2012] Acute toxicity, antipyretic and antinociceptive study of the crude saponin from an edible vegetable: *Vernonia amygdalina* leaf. *Int J BiolChem Sci.* 6:1019-1028.

ARTICLE

IMPACT OF ARENGA PINNATA ADMINISTRATION COMBINED WITH TAI-CHI GYMNASTICS ON BONE DENSITY IN MENOPAUSAL WOMEN

Safrina*, Sri Hernawati Sirait

Program Studi Kebidanan Pematangsiantar, Poltekkes Kemenkes, Sumatera Utara, Medan, INDONESIA



ABSTRACT

Various tissues are present in the human body and one of the most important tissues which play a pivotal role in movement, strength and stability is the bone. Bone like every other living tissue constantly has to be repaired and renewed also occurs hand in hand. It is well established that there is gradual loss of bone with aging in adults, but major bone loss in women occurs with loss of oestrogen at the menopause. Various ways have been employed towards reduction of symptoms accompanying osteoporosis a notable one is the relaxation of footwork (stretching) included in relaxation techniques. Apart from relaxation techniques there are also other ways to reduce pain and an example of this is the 'tai-chi gymnastics'. *Arenga pinnata* is a type of palm tree growing in tropical forests and is considered as one of the most diverse multipurpose tree species. In this study the effect of the effect of combination of *Arenga pinnata* and Tai-Chi gymnastics on bone density was assessed. From this study it was concluded that bone density change was noticed after intervention using combination of Tai-Chi gymnastic with *Arenga pinnata* was carried out and the change was statistically significant. Therefore it can be concluded that administration of *Arenga pinnata* with Tai-Chi gymnastics has a significance effect on improving bone density in postmenopausal women.

INTRODUCTION

Various tissues are present in the human body and one of the most important tissues which play a pivotal role in movement, strength and stability is the bone [1]. Bone like every other living tissue constantly has to be repaired and renewed also occurs hand in hand. This process is continuous because the daily damages although microscopic that occurs within the bone. The process by which this ours is called bone turnover and is carried and certain cells in the bone are responsible for this [2]. The most important of them been the one set (osteoclasts) that are involve in digging up bone whilst the other set (osteoblasts) lay down new bone. Like every other process within the body this process is well balanced and the activities of one cell does not out run that of the other. If there is a relative increase in bone removal, which is notable after the age of menopause in women bone tissues loss become progressively increasing and bones become thinner [3, 4]. It is well established that there is gradual loss of bone with aging in adults, but major bone loss in women occurs with loss of oestrogen at the menopause. The drastic loss of estrogen hormone that occurs after menopause increases the risk of decreased bone density which is often times accompanied by increased calcium wasted excretion from a woman's body. This will gradually cause a decrease in bone density or a reduction in the mass of bone tissue per unit volume (g/cm^2), so the bones become thinner, more fragile and contain less calcium or bone more porous, a commutation of processes known as osteoporosis [5]. Osteoporosis which is known as the thin bone disease currently is estimated to affect more than three million people in the UK with postmenopausal women being the most affected [6, 10].

Various ways have been employed towards reduction of symptoms accompanying osteoporosis a notable one is the relaxation of footwork (stretching) included in relaxation techniques. Apart from relaxation techniques there are also other ways to reduce pain and an example of this is the 'tai chi gymnastics', which is noted for its benefit of increasing muscle tone and strengthen muscle-muscle weakness enabling joints to become more flexible muscles which will result on the long run participants in this activity ability to feel more comfortable with pain due to the reduction in threshold of pain accomplished. *Arenga pinnata* is a type of palm tree growing in tropical forests and is native to the Indo-Malayan archipelago, easily found in South and Southeast Asia [7]. Among the 3000 palm species of the tropics and subtropics categorized as multipurpose trees, the *Arenga pinnata* tree is considered as one of the most diverse multipurpose tree species under culture, and the only one attracting widespread economic interest [8, 9]. The aim of this study is to impact of Tai-Chi gymnastics with *Arenga pinnata* administration on bone density in menopausal women.

MATERIALS AND METHODS

For this study, 50 postmenopausal women were recruited. The inclusion criteria were that they should be postmenopausal and should also be involved in tai chi gymnastics while those postmenopausal women that didn't meet this requirement were excluded from this study. The selected 50 women were then divided into two groups respectively for this study.

Group 1: These consist of 25 postmenopausal women who served as the control group and only participated in Tai-Chi gymnastic without been administrated *Arenga pinnata*.

KEY WORDS

Tai-Chi, Bone density, menopause, osteoporosis

Received: 13 May 2018
Accepted: 15 May 2018
Published: 10 July 2018

*Corresponding Author

Email:safrinausu@yahoo.com
Tel.:+62-85883439716

Group 2: These consist of 25 postmenopausal women who served as the intervention group and participated in Tai-Chi gymnastic and *Arenga pinnata* was also administrated to them.

In this study the Tai-Chi gymnastics is performed every three weeks for 3 months and kaling is given 100 grams / day for three months to the intervention group while the control group performed Tai-Chi gymnastics only every three weeks for three months without taking *Arenga pinnata*. After the period of 3 months elapsed, the administration of *Arenga pinnata* was stopped and both groups were assessed. Univariate analysis was done in this study aims to see the description of the frequency distribution of respondent characteristics studied in both groups namely tai chi gymnastics and Tai-Chi gymnastics + *Arenga pinnata* while bivariate analysis differences in bone density in both groups of respondents was also assessed.

Written consent was taken from all the participating subjects and the work was approved by the ethical approval committee of Ministry of health of republic of Indonesia.

RESULTS

[Table 1] show characteristics of both groups of participants in this study while [Table 2] shows bivariate analysis differences in bone density in both groups of respondents and for [Table 2], the statistical test results showed no difference between the two groups ($p > 0.05$). [Table 3] shows that the average bone density level before intervention in the tai-chi gymnastic group is lower at 44.33 ± 11.96 BQI than the Tai-Chi + *Arenga pinnata* gymnastics group which is 53.33 ± 12.87 BQI with the difference of 8.99 BQI and the statistical test results showed that there was a difference between the two groups ($p < 0.05$). [Table 4] shows the differences in bone density before and after intervention in the Tai-Chi gymnastic and the results of statistical tests showed there were differences before and after Tai-Chi gymnastics ($p < 0.05$). These results can be seen in the following [Table 1] description below.

Table 1: Characteristics of both groups of research respondents

Variable	Tai- chi gymnastic (n=25) (Average \pm SD)	Tai-chi gymnastic and <i>Arenga pinnata</i> (n=25) (Average \pm SD)
Age	59.92 \pm 3.88	58.96 \pm 5.76
Body weight	58.80 \pm 5.39	60.48 \pm 5.92
Height	153.8 \pm 4.08	154.6 \pm 4.29
Initial menopause age	13.76 \pm 1.29	13.44 \pm 1.16
Final menopausal age	50.68 \pm 3.57	50.2 \pm 3.36
Density level Before gymnastics	41.24 \pm 12.66	42.47 \pm 11.10
Density levels After gymnastics	44.33 \pm 11.96	53.33 \pm 12.87

Table 2: Differences in bone density in both groups prior to the intervention

Group	n	Average \pm SD (BQI)	Average difference (IK 95%)	p
Tai-Chi gymnastic	25	41.24 \pm 12,66	1.23 (5.54 - 8.00)	0.716
Tai-Chi+ <i>Arenga pinnata</i>	25	42.47 \pm 11,10		

Table 3: Average group bone density before intervention

Group	N	Average \pm SD (BQI)	Average difference (IK 95%)	p
Tai-Chi gymnastics	25	44.33 \pm 11,96	8.99 (1.93– 16.06)	0.014
Tai-Chi exercise + <i>Arenga pinnata</i>	25	53.33 \pm 12.87		

Table 4: Differences in bone density before and after intervention in the tai chi gymnastic group

	N	Average \pm SD (BQI)	Average difference (IK 95%)	p
Before Tai-Chi gymnastic	25	41.24 \pm 12.66	3.09 (1.85 - 5.16)	0.000
After Tai-Chi exercise	25	44.33 \pm 11.96		

CONCLUSION

The administration of *Arenga pinnata* in combination with Tai-Chi gymnastics had a significance effect on improving bone density unlike when tai chi gymnastics is done alone. This finding is of benefits in making treatment of low bone density in postmenopausal women easy. Therefore, it is recommended that this should be practice and this extra benefit should be maximize towards preventing or delaying osteoporosis in postmenopausal women. Also due to the limited research in this field, it is also recommended that more

research should be done to further authenticate this perceive benefits of combination of Tai-Chi gymnastics with *Arenga pinnata* on bone density improvement in postmenopausal women.

CONFLICT OF INTEREST

Nil

ACKNOWLEDGEMENTS

In the current research patient written consent forms were signed from the participating individuals. We are thankful to the ethical approval committee of Ministry of health of republic of Indonesia for granting us ethical approval letter No: 015/KEPK/POLTEKES KEMENKES MEDAN/2017 to carry out the research.

FINANCIAL DISCLOSURE

Self-funded

REFERENCES

- [1] Gerard J, Tortora BHD.[2012] The skeletal system: Bone tissue. In Principles of Anatomy and Physiology, 13rd ed.; Wiley: Hoboken, NJ, USA, pp. 182–207.
- [2] Burt LA, Greene DA, Naughton GA. [2017] Bone health of young male gymnasts: A systematic review. *Pediatr Exerc Sci*, 29(4):456-464
- [3] Batoon L. Millard SM, Raggatt LJ, Pettit AR. [2017] Osteomacs and Bone Regeneration. *Curr. Osteoporos. Rep.* 15:385–395.
- [4] Baldwin JG, Wagner F, Martine LC, et al. [2017] Periosteum tissue engineering in an orthotopic in vivo platform. *Biomaterials*. 121:193–204.
- [5] Pinheiro MM, Reis N, Machado ET, Felipe FS, Yang O, SzejnfeldJH, et al.[2010] Risk factors for osteoporotic fractures and low bonedensity in pre and postmenopausal women. *Rev SaudePublica*. 44:479–85.14.
- [6] Osteoporosis: bone health following the menopause, Women's Health Concern. 2017. (<https://www.womens-health-concern.org/help-and-advice/factsheets/osteoporosis-bone-health-following-menopause/>) Accessed on April, 2018)
- [7] Sahari J, Sapuan SM, Zainudin ES, Maleque MA. [2012] Sugar palm tree: A versatile plant and novel source for biofibres, biomatrices, and biocomposites. *Polymers from Renewable Resources*. 3(2): 61-77.
- [8] Yuldiati M, Saam Z, Mubarak. [2016] Community local wisdom in utilizing arenga palm trees in Siberakun Village, BenaiSubdistrict, Kuantan Singingi District. *Dinamika Lingkungan Indonesian*. 3(2): 77-81.
- [9] Iskandar J. [2016] Ethnobiology and Cultural Diversity. *Umbara: Indonesian. J Anthropol*. 1 (1): 27-42.
- [10] Alendronate, etidronate, risedronate, raloxifene, strontium ranelate and teriparatide for the secondary prevention of osteoporotic fragility fractures in postmenopausal women; NICE Technology Appraisals, January 2011. (<http://nicedsu.org.uk/appraisal-specific-projects/osteoporosis>)

ARTICLE

EFFICIENT SOLAR PHOTOCATALYST BASED ON TiO_2 /CORN SILK NPS COMPOSITE FOR REMOVAL OF A TEXTILE AZO-DYE FROM AQUEOUS SOLUTIONHayrunnisa Nadaroglu^{1,2*}, Asghar Lesani², Seyedeh Sara Soleimani², Aynur Babagil², Azize Alayli Gungor^{2,3}¹Ataturk University, Erzurum Vocational Training School, Department of Food Technology, Erzurum, TURKEY²Ataturk University, Faculty of Engineering, Department of Nano-Science and Nano-Engineering, Erzurum, TURKEY³Ataturk University, Erzurum Vocational Training School, Department of Chemical Technology, Erzurum, TURKEY

ABSTRACT

Background: The results of investigations on a new advanced oxidation process regarding a new embedded heterogeneous photocatalyst on corn silk/titanium dioxide nanoparticules composite are presented. **Methods:** UV-VIS-spectroscopy, Scanning electron microscopy (SEM), Fourier-transform IR spectrometry (FT-IR), and X-ray powder diffraction (XRD) were applied to characterize the effect of functionalization, structure, surface morphology and optical properties of composites and mineralization of pollutants. **Results:** The present work confirmed the role of corn silk/titanium dioxide NPs as a factor which not only activated the catalyst with UV light but also raised the adsorption of species by increasing the active surface area. A small UV-shift of band gap values regarding that of commercial photo-active TiO_2 was detected as consequence of the quantum size effect, suggesting that photocatalytic experiments should be performed under UV-radiation assistance. **Conclusion:** The synthesized corn silk/titanium dioxide (TiO_2)NPs showed good activity in the photocatalytic oxidation of Direct blue 15 (DB 15) achieving conversions higher than 90% within 30 s.

INTRODUCTION

Our world is faced with a huge problem of environmental pollution due to the rapid growth and industrialization influence results. Dyes and pigments are the most important source of water pollutants. The dyeing process as well as consume a large amount of water is an important factor polluting rivers [1]. Reactive dyes are especially used in textiles, paper, wool, cotton, silk, printing and leather industries. Because these dyes were discarded in large amounts and toxic, they cause great environmental pollution problems [2,3]. Every year, 80 000 tons of reactive dyes are produced for different industries and they are the source of environmental pollution. Reactive azodyes are generally synthetically produced and aromatic and they includes complex molecular structures such as benzene, naphthalene, anthracene comprises to luene and xylene [4]. Reactive dyes are the largest class of synthetic dyes with high ability to dissolve in water and they are usually resistant to bio degradation process [5]. The discharge of these colored compounds into the environment causes considerable non-aesthetic pollution and serious health risks [6].

Physico-chemical processes such as adsorption [7, 8], ion exchange [9] and membrane filtration [10] are expensive, insufficient, and these processes can be applied to a large amount of dye waste water. Instead of this method, the biodegradation, bio accumulation and biosorption techniques are used these methods are too weak in terms of impact [11].

Another dye removal method is enzymatic process. However, in this method, enzymes are inhibited at different pHs, temperatures and in the presence of inhibitors and they aren't effective [12]. Chemical methods such as chemical oxidation [13], electro chemical degradation [14] and ozonation [15] are quite effective methods. However, these generally used techniques are very expensive and lead to the formation of toxic byproducts. Especially as the oxidizing agent used as the hypochlorite is halides' decolorizes organic toxic substances. In addition, the pre-treatment requirements for the implementation of these methods constitutes a significant draw back [16].

Recently, nano particles hold an important place in the presence of photocatalytic degradation, due to the cheap and effective. In addition, through this process, toxic azo dyes are also converted to CO_2 , water and mineral acid. This process is performed generally in the presence of a semiconductor metal and UV light ($\lambda < 400 \text{ nm}$). TiO_2 which is widely used is a photo catalyst which is easily obtainable, inexpensive, non-toxic and stable [17]. TiO_2 nanoparticles have more photocatalytic activity in the liquid medium and collecting of them is extremely difficult from their aqueous environment. After using, TiO_2 NPs are often left in a freely into the environment, and they can easily penetrated to membranes of biological microorganisms and plants and they cause their death. For this reason, to be immobilized on a support material of TiO_2 NPs photo catalyst is a big advantage. Glass, silica, quartz, activated carbon, mesoporous clays, and polymeric materials have been used as support material for TiO_2 NPs [18]. Most materials with granule-shaped reduce the photo catalysis performance because of reducing the effect of UV photon [18]. TiO_2 is not available any research in literature related to immobilization TiO_2 NPs with corn silk. Corn silk is non-toxic, bio-degradable and a fibrous material. In this study, to be immobilized TiO_2 NPs onto corn silk fiber structure and usability of this material in degradation of DB 15 azo dye was investigated.

KEY WORDS

Corn silk, titanium dioxide NPs, textyl dye, Direct blue 15

Received: 17 January 2018

Accepted: 31 January 2018

Published: 1 Aug 2018

*Corresponding Author

Email:

hnisa25@atauni.edu.tr

Tel.: 0-90-442-2311818

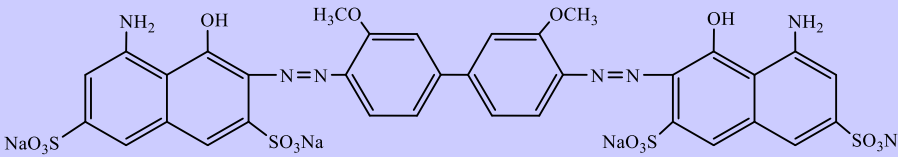
Fax: +90-442-2360982

MATERIALS AND METHODS

Chemicals

Direct blue 15 (DB15), sodium hydroxide (NaOH), hydrochloric acid (HCl), Sodium hypochlorite (NaClO), Titanium dioxide Nanoparticles (TiO_2 NPs) (<20 nm) were purchased from Sigma/Aldrich Co. The chemical characteristics and structures of DB15 were summarized in Table 1. Distilled water was used for all the tests performed (GFL 2004).

Table 1: General characteristics of Direct blue 15 dye

Direct blue 15 (DB15)	
Chemical formula	$\text{C}_{34}\text{H}_{24}\text{N}_6\text{O}_{16}\text{S}_4\text{Na}_4$
Chemical structure	
Molar mass (g mol^{-1})	992.80
λ_{max} (nm)	596

Supply and preparation for analysis of corn silk material

Corn silk (CS) is obtained from local corn seller. 25 g corn silk sample was taken and added to 250 mL, 0.5 M NaClO solution. Then, this mixture was incubated in a water bath (80 °C) for 1 hour. Corn silk then washed thoroughly with 250 ml of pure water and corn silk was incubated in the same conditions with 1 M NaOH solution. Then, corn silk was thoroughly washed with pure water and dried in oven at 60 °C for 8 hours. Dried corn silk sample was fractionated with pure water in the steel blender. Then, 0.2 g TiO_2 NPs were added to obtained mixture and incubated for 2 h in an ultrasonic bath environment at 60 °C for immobilizing TiO_2 NPs onto silk corn. Then, TiO_2 immobilized corn silk was separated from the supernatant. TiO_2 immobilized corn silk support material was washed 5 times with pure water and unbound TiO_2 NPs were removed. This obtained TiO_2 immobilized Corn silk support material was dried in the oven at 60 °C for 8 hours and it was used in all studies.

Characterization methods of the CS and TiO_2 -IML CS

The Scanning Electron Microscopy (SEM) images and chemical analysis at Energy Dispersive X-ray (EDX) of nanoparticles were recorded with a Zeiss Sigma 300 field emission SEM. The analysis was performed by mounting CS and TiO_2 -IML-CS samples onto pin type SEM stubs using carbon/platinum adhesive tabs and was coated with carbon by electro deposition under vacuum prior to analysis to enhance the surface conductivity.

X-ray diffractogram (XRD) of CS and TiO_2 -IML-CS, before and after dye treatment, was undertaken using a PANalytical Empyrean model XRD at $\text{Cu-K}\alpha$ radiation ($\lambda=1.54 \text{ \AA}$). The analysis of dried CS and TiO_2 NPs-IML-CS were carried out continuous scans from 10 to 100° at 2° scan rate at 2 θ min⁻¹ in ambient air.

FTIR analysis of DB 15 dye and TiO_2 NPs-IML-CS, before and after dye treatment, was recorded using a Vertex 80 Model FTIR Frontier spectrophotometer with attenuated total reflection (ATR) technique in the 4000-400 cm^{-1} region.

Preparation of dye solutions and UV-vis analysis

The stock solutions of DB 15 were prepared in 50 mg/L concentration and used by diluting with deionized water further experiments. Before experiments, desired pH of the solution was adjusted by Thermo scientific Orion 4 Star digital pH meter with diluted HCl or NaOH solutions. The UV-vis spectra of dye solutions were recorded from 200 to 900 nm using an Epoch Microplate Spectrophotometer equipped with a quartz cell of 1.0 cm path length. The concentrations of samples were quantified by measuring the absorption intensity at maximum wavelength.

Batch experiments

Direct blue 15 azo dyes degradation was carried out in a closed system consisting of a magnetic stirrer and UV-C lamp. For this purpose, the reaction medium was prepared by adding 25 mL (50 mg / L) DB 15 azo dye and 0.4 g of TiO_2 -NPs IML- CS sample in a 250 ml beaker. The same tests were performed for CS and TiO_2 NPs samples, respectively. Distilled water was used as a blank sample. The dye removal efficiency was calculated using the following equation:

$$\text{Removal}(\%) = \frac{C_0 - C_t}{C_0} \times 100 \quad (1)$$

where Removal (%) was the dye removal efficiency, Co (mg/L) was the initial dye concentration, and Ct (mg/L) was the concentration of dye at t min [19].

Effect of some parameters

Degradation of DB15 azo dyes was followed by measuring absorbance at 596 nm. In order to determine the content time, degradation reaction in UV system was followed during 10 min. For this purpose, samples taken periodically from reaction medium measured against distilled water and degradation% was calculated using the equation (1).

Also, the effects of pH and stirring speed on the photo degradation of DB15 were investigated. For this purpose, the pH of DB15 azo dye was adjusted using a pH meter and 0.01 N HCl / NaOH solutions at pHs 3-10. In each pH value, absorbance changes were monitored at 596 nm by establishing the same experimental.

The effect of stirring speed

In order to monitor the effect of stirring speed; 0.4 g corn silk was added to 25 mL, DB15 azo dye at 50 mg / L concentration solution and reactions were occurred at 25 °C, and pH 3.0 and at 100, 200, and 300 rpm, respectively. Absorbance values were recorded at 596 nm against distilled water.

The effect of support material

In order to investigated of the effect of support material onto removal of DB15, different reactions were performed between 0.1 and 0.8 g TiO₂-IML-CS, respectively.

The effect of dye concentration

The effect of dye concentration on the photocatalytic degradation of DB15 azo dye was investigated following the prepared reactions in the same conditions (pH 3.0, 25 °C, 300 rpm) and at 5, 25, 50, 75, 100, 150 and 200 mg/L DB15 dye concentrations [20].

Reusability experiments for TiO₂ NPs immobilized corn silk

The removal of DB15 was performed 10 cycles to assess the potential reusability of TiO₂-IML-CS NPs at an initial concentration of 50 mg/L. Before each cycle, TiO₂-IML-CS NPs pieces were washed three times with distilled water. All tests were done in triplicates and the data referred in this paper is the mean value [21].

RESULTS AND DISCUSSION

Characterization of support material

The surface morphology of TiO₂ nanoparticles and TiO₂ nanoparticles immobilized corn silk after removal of DB15 azo dye samples are given in [Fig. 1]. Although a quantity of TiO₂ nanoparticles agglomerates in [Fig. 1A], it appears to be immobilized TiO₂ NPs on the corn silk fibrous structure very well in [Fig. 1B]. Corn silk fiber structure in the photocatalytic effect of TiO₂ NPs can be understood from [Fig. 1B] can show very easily. Thus, the TiO₂ NPs can be easily removed from the reaction medium as a way to be able to participate effectively in both the photocatalytic reaction.

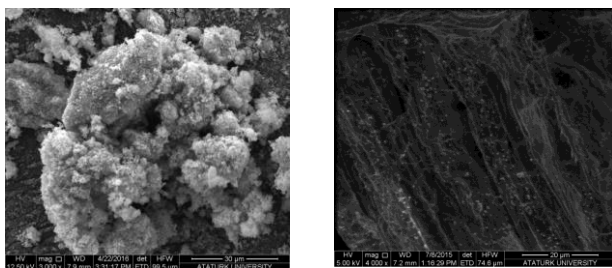


Fig. 1: SEM images of (A) TiO₂ nanoparticles and (B) TiO₂ nanoparticles immobilized corn silk after DB15 dye removal.

FTIR Spectra of the corn silk fibers [Fig. 2] showed the FTIR spectra of CS, TiO₂ NPs, TiO₂ NPs-IML-CS and TiO₂ NPs-IML-CS+DB15. In the FTIR spectrum of CS, the IR spectra had peaks at ca.1650-1700 cm⁻¹ which was attributed to the C=O stretching and 2600-3000 cm⁻¹ which correspond to the ester C=O stretching vibration and carboxylic acid O-H [22].

The peaks at 3400 and 1639.5 cm⁻¹ in the spectra are due to the stretching and bending vibration of the -OH group. In the spectrum of pure TiO₂, the peaks at 596.0 cm⁻¹ show stretching vibration of Ti-O and peaks at 1060.84 cm⁻¹ shows stretching vibrations of Ti-O-Ti [23].

The FTIR spectrum of TiO₂ NPs-IML-CS after treatment on DB15 shows the peak at 3410.13, 2920.20 and 2380.1. The band at 3410.13 shows -NH₂ group aliphatic and aromatic group, 2920.20 shows C-H, aliphatic group, 2380.1 shows C-N azo group and 1047.3 cm⁻¹ shows that OR aromatic group.

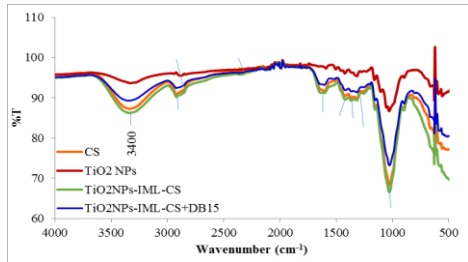


Fig. 2: FT-IR spectra of the CS; TiO₂ NPs; TiO₂ NPs-IML-CS and TiO₂ NPs-IML-CS+DB15.

When it was compared nature CS and immobilized TiO₂ NPs-IML-CS peak

According to CSPDS card with numbered 21-1272; the obtained peak at 2 theta = 25° (101) was belong to TiO₂ NPs (anatase). Also, at the 2Theta=32°, 48°, 55° and 62° peaks were approved that TiO₂ NPs were bound to CS fibers.

When the looking at the XRD diagrams of TiO₂ NPs; TiO₂ NPs-IML-CS and TiO₂ NPs-IML-CS+DB15:

It was observed that all immobilized TiO₂ NPs were reacted with DB15 azo dye during Photo reaction under UV light. Therefore, it was not seen all peaks related to TiO₂ in the TiO₂ NPs-IML-CS+DB15 and this event confirmed that the photo degradation was done [Fig.3].

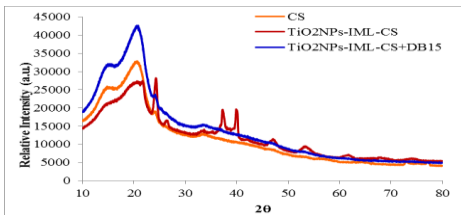


Fig. 3: XRD diagram of CS; TiO₂ NPs; TiO₂ NPs-IML-CS and TiO₂ NPs-IML-CS+DB15.

Effect of time

To confirm the photo degradation of DB 15 azo dye, the absorbance of the samples was analyzed at several time points during the reaction. As seen from [Fig. 4], the there was a 97.05% reduction in the presence of TiO₂-CS-IML when the immobilized TiO₂ onto CS fibers were allowed to degrade DB-15 dye (50 ppm) for 30 sec. When the only corn silk was used, it was achieved 2% and 5% removal of DB 15 azo dye for 30 sec 10 min, respectively. Too effectively removal of DB15 azo dye at 30 sec with TiO₂ NPs-IML-CS, it will be brought great benefits in terms of low cost, energy and time on an industrial scale [24].

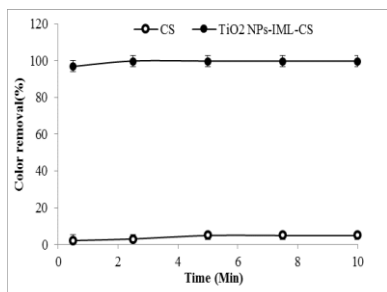


Fig. 4: The photocatalytic removal rate of DB15 at a concentration of 50 mg/L, 25°C and 300 rpm.

Effect of pH

pH is an important parameter for photo degradation reactions taking place on the surface of TiO₂ nanoparticles. pH variation can in fact influence the adsorption of dye molecules onto the TiO₂ surfaces [25]. The effect of solution pH was studied in the range of 3 to 10 for the DB 15 azo dyes under study using both CS and TiO₂-IML-CS. [Fig. 5] showed the variation on the efficiency photocatalytic degradation of DB15 at different pH values. Photo degradation was higher in acidic media (pH 3 to 5) using TiO₂-IML-CS

for 30 sec, with degradation rates of 99 and 95%, respectively. Degradation rate of DB 15 azo dye as UV catalytically using TiO₂-IML-CS for 30 sec (s) was obtained at 90.0%. Up to a pH value of 7, the dye degradation efficiency decreased to 81.12% using TiO₂-IML-CS. Above pH 7, the degradation continued to decrease to about 80.78% at pH 10 [25].

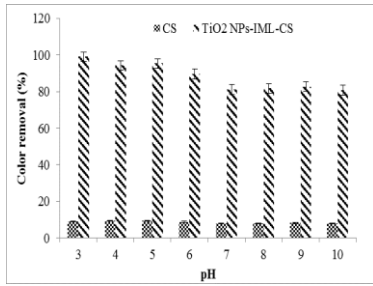


Fig. 5: The effect of pH on the photocatalytic removal rate of DB 15 azo dye (pH:3.0, 25°C, 300 rpm).

TiO₂ NPs-IML-CS surface is positively charged in acidic reaction medium (pH<7.0), whereas under alkaline conditions (pH>7.0) it is negatively charged [26]. Seeing the structure of DB 15 azodye [Fig. 6], a positive charge excess in the TiO₂ surface supports a strong interaction with four SO₃-groups of the dye [Fig. 6A]. A negative charge excess promotes there pulsing of the DB 15 azodye by the TiO₂ NPs-IML-CS surface, reducing the catalytic activity of this photo catalyst [Fig. 6B]. These results suggest that the influence of the initial pH of the solution on photo catalysis reaction kinetics is due to the amount of the dye adsorbed on TiO₂ NPs-IML-CS [25,27]. This hypothesis supports with a reaction occurring at TiO₂ NPs-IML-CS surface and not in the solution, close to the surface.

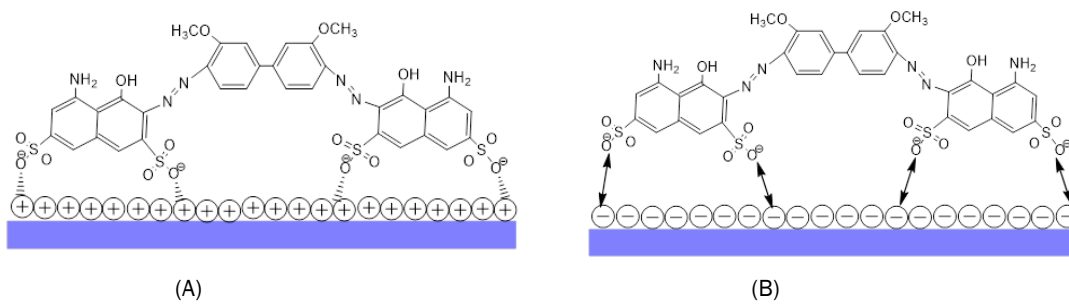


Fig. 6: Schematic reaction mechanism of DB 15 and TiO₂NPs IML CS (A) acid sites and (B) basic sites.

The effect of stirring speed

The effect of stirring speed on the photo degradation reaction of DB15 azo dye was investigated using stirring speed from 100 to 300 rpm using dye concentration of 50 mg/L, contact time 30 s, and temperature was 25°C. It was shown from [Fig. 7] that with increasing of the stirring speed photo degradation of DB 15 was increased from aqueous solution. This increase in degradation of DB15 azo dye reached a maximum at 300 rpm as 99.76% removal rate using TiO₂-IML-CS. The increase in photo degradation of DB15 may be increase the contact between the surface of TiO₂-IML-CS and DB 15 with increasing the stirring speed [28].

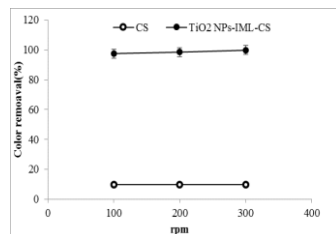


Fig. 7: The effect of stirring speed on the photocatalytic removal rate of DB 15 azo dye (pH:3.0, 25°C, 30s).

Effect of dye concentration

The effect of the initial concentration of DB 15 on the photo degradation of the dye under UV photon was determined. The obtained results are presented in [Fig. 8]. When initial dye concentration effect on the removal efficiency is also investigated, it is seen that at Fig. 8 low initial dye concentration values are effective for DB 15 dye removal. When the initial dye concentration decreases 200 to 50 mg/L the removal efficiency of DB 15 increases from 71.13% to 99.76%. The results indicate that the photo degradation in rate of DB 15 dye strongly depends on the initial dye concentration. The efficiency of photo degradation of DB 15 dye decreased with increase of the initial dye concentration [29].

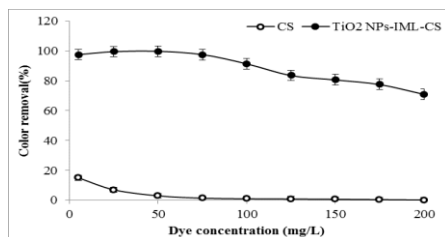


Fig. 8: The effect of dye concentration on the photocatalytic removal rate of DB 15 azo dye (pH:3.0, 25 °C, 300 rpm, 30 s).

The effect of photo catalyst amount

The effect of TiO₂ NPs-IML-CS amount was also investigated. The obtained results are presented in [Fig. 9]. The results were indicated that the TiO₂ NPs-IML-CS amount increased 0.05 to 0.75 g/ 50 mL, removal efficiency of DB 15 increases from 89.25 to 99.76%. Using CS and TiO₂ NPs-IML-CS, DB 15 with 0.4 g/50 mL of photo catalysts showed rates of degradation of 99.76 and 7%, respectively. It was observed that the efficiency of photo degradation of DB 15 azo dye decreased with increasing of the initial photo catalyst amount [30]. Therefore, photo catalyst prevented UV rays reaching the surface of the DB 15. Therefore, photo catalyst prevented the UV rays reaching the surface of DB 15 azo dye.

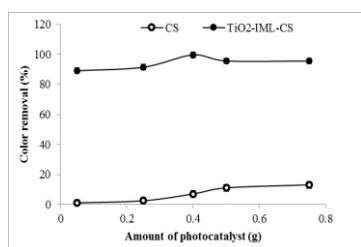


Fig. 9: The effect of photo catalyst amount on the photocatalytic removal rate of DB 15 azo dye (pH:3.0, 25 °C, 300 rpm, 30 s).

Reusability

The reusability of TiO₂ NPs-IML-CS was investigated in order to establish the stability [Fig. 10] while studying reuse of photo catalyst; all parameters including irradiation time (30 s), pH: 3.0, DB 15 concentration (50 mg/L), and amount of and photo catalyst (0.4 g) were kept constant. The photo catalyst was separated from the solution mixture through filtration. The recovered photo catalyst was washed with distilled water and reused ten times as in the previous degradation process. According to the obtained results, after using of 6 cycles, it was identified 73.32% removal of DB-15 azo dye. Results showed no significant reduction in photocatalytic performance in photodegrading DB 15 at the first six times, thus this indicated the stability of TiO₂ NPs-IML-CS as a photo catalyst [12].

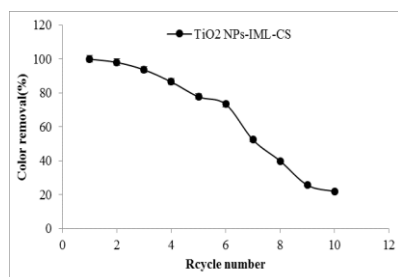
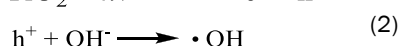
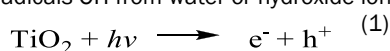
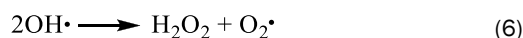
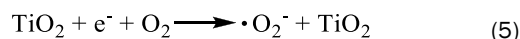
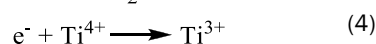


Fig. 10: The effect of reusability capability of TiO₂ NPs-IML-CS on the photocatalytic removal rate of DB 15 azo dye (pH:3.0, 25 °C, 300 rpm, 30 s).

Reaction mechanism of photo catalytic DB15 dye degradation

Hetero generous photo catalysis for the treatment of azodyes appears as an interesting technique. Indeed, titanium dioxide (TiO₂) activation under UV irradiation ($\lambda < 390$ nm) allows the generation of highly reactive free radicals OH from water or hydroxide ions as follow:





These free radicals can then react with the DB15 azo dye adsorbed on the surface of TiO_2 until DB 15 total mineralization. The photocatalytic mechanisms of TiO_2 are assumed as follow [Fig. 11A] (Birhanli and Yesilada 2006). The ambient temperature and the possible use of solar UV are the advantages of photo catalysis; moreover, TiO_2 is not toxic. The reaction mechanisms of TiO_2 photocatalytic oxidation of azodyes was similar to the bio degradation process of oxidation of azodyes with $\cdot\text{OH}$ radical. One of the reaction mechanisms of oxidation of azodyes that react with $\cdot\text{OH}$ radical was proposed as follows [Fig. 11B] [31].

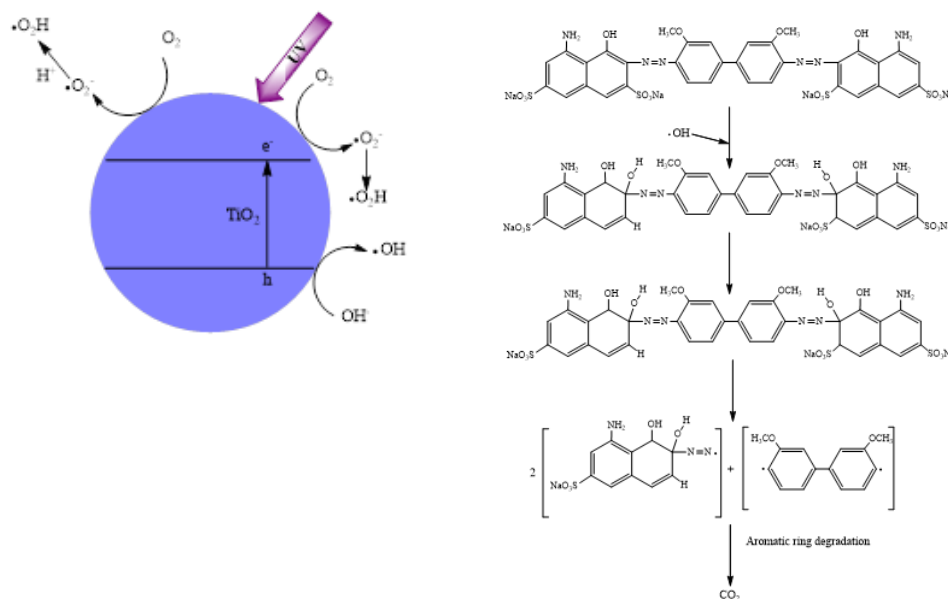


Fig. 11: Photo catalytic oxidation reaction mechanism of TiO_2 for DB 15 azodyes removal.

CONCLUSION

The photo catalytic degradation of Direct blue 15 (DB 15) azo dye mediated by TiO_2 NPs-IML-CS was successfully achieved. Before and after treatment with dye, the XRD of CS and TiO_2 NPs-IML-CS showed that modified CS with TiO_2 NPs reacted with DB 15 azo dye very high level. The results of UV-vis and FTIR spectras showed that de colorization of DB 15 was confirmed the cleavage of azo bonds of molecule. Three main steps were proposed for the de colorization mechanism using TiO_2 NPs-IML-CS (a) the cleavage of the azo bonds by reduction of DB15 dye /oxidation of TiO (b) adsorption of anionic dye on the TiO_2 NPs-IML-CS (c) When the used TiO_2 NPs-IML-CS, TiO_2 NPs could be joined the photocatalytic reaction and then easily removed from the reaction medium. In designing the dye removal experiments with low and high level of independent variables such as CS amount, initial dye concentration, temperature and pH, the amount of DB 15 azo dye removal (%) was obtained as response. According to obtained results, the best reaction medium for DB 15 removal (%) was determined as 0.4 g/50 mL TiO_2 NPs-IML-CS amount, 50.0mg/L initial dye concentration, pH 3.0 and 25.0 °C temperature. There cycling of TiO_2 NPs-IML-CS can be performed and it was observed that with the photo catalyst being able to be adequately used five times. According to best solution, the maximum DB 15 removal percent is 99.76%.

CONFLICT OF INTEREST

There is no conflict of interest.

ACKNOWLEDGEMENTS

To prepare proposed methodology paper on "Efficient Solar Photo catalyst Based On TiO_2 /Corn Silk Nps Composite For Removal of A Textile Azo-Dye From Aqueous Solution" has been prepared by Prof.Dr. Hayrunnisa Nadaroglu, Prof. Dr. Azize ALAYLI GUNGOR and Dr. Asghar Lesani. I would like to thank my vocational school as well as my whole department, parents, friends for their support.

FINANCIAL DISCLOSURE

None

REFERENCES

- [1] Barakat H. [2010] Adsorption and photo degradation of procion Yellow H-Exl Dyes in textile wastewater over TiO₂ Suspension. Proc International Water Technology Conference, Cairo, Egypt.
- [2] Zollinger H. [1989] Color Chemistry - Synthesis, Properties and Applications of Organic-Dyes and Pigments - Zollinger H. Leonardo. 22(3-4):456-456.
- [3] Chatterjee S, Lim SR, Woo SH. [2010] Removal of Reactive Black 5 by zero-valent iron modified with various surfactants. Chemical Engineering Journal. 160(1):27-32.
- [4] Vijayaraghavan J, Basha SJS, Jegan J. [2013] A review on efficacious methods to decolorize reactive azo dye J Urban Env Eng. 7(1):30-47.
- [5] Erdal S, Taskin M. [2010] Uptake of textile dye Reactive Black-5 by *Penicillium chrysogenum* MT-6 isolated from cement-contaminated soil. Afr J Microbiol Res. 4:618-625.
- [6] Ohashi T, et al. [2012] An improved method for removal of azo dye orange ii from textile effluent using albumin as sorbent molecules. 17(12):14219-14229.
- [7] Chatterjee S, et al. [2009] Congo red adsorption from aqueous solutions by using chitosan hydrogel beads impregnated with nonionic or anionic surfactant. Bio resource Technology. 100(17):3862-3868.
- [8] Chatterjee S, Lee MW, Woo SH. [2009] Influence of impregnation of chitosan beads with cetyl trimethyl ammonium bromide on their structure and adsorption of congo red from aqueous solutions. Chemical Engineering Journal. 155(1-2):254-259.
- [9] Labanda J, Sabate J, Llorens J. [2009] Modeling of the dynamic adsorption of an anionic dye through ion-exchange membrane adsorber. Journal of Membrane Science. 340(1-2): 234-240.
- [10] Ahmed S, Siddiqui HA. [2015] Screening and assessment of laccase producing trichoderma species isolated from different environmental samples. Journal of Animal and Plant Sciences. 25(3):606-610.
- [11] Wang H, et al. [2009] Biological de colorization of the reactive dyes Reactive Black 5 by a novel isolated bacterial strain *Enterobacter* sp EC3. J Hazard Mater. 171(6):654-659.
- [12] Kalkan E, et al. [2014] Removal of textile dye Reactive Black 5 from aqueous solution by adsorption on laccase-modified silica fume. Desalination and Water Treatment. 52(31-33):6122-6134.
- [13] Osugi ME, et al. [2009] Comparison of oxidation efficiency of dispersed dyes by chemical and photo electro catalytic chlorination and removal of mutagenic activity. Electrochim Acta. 54:2086-2093.
- [14] Yi FY, Chen SX, Yuan C. [2008] Effect of activated carbon fiber anode structure and electrolysis conditions on electrochemical degradation of dye wastewater. Journal of Hazardous Materials. 157(1):79-87.
- [15] Moussavi G, Mahmoudi M. [2009] Degradation and biodegradability improvement of the reactive red 198 azo dye using catalytic ozonation with MgO nanocrystals. Chemical Engineering Journal. 152(1):1-7.
- [16] Danis U, Gurses A, Canpolat N. [1999] Removal of some azo dyes from wastewater using PAC as adsorbent. Fresenius Environmental Bulletin. 8(5-6):358-365.
- [17] Mahmoodi NM, et al. [2005] Decolorization and aromatic ring degradation kinetics of Direct Red 80 by UV oxidation in the presence of hydrogen peroxide utilizing TiO₂ as a photocatalyst. Chem Eng J. 112:191-196.
- [18] Zhang S, et al. [2010] TiO₂/SBA-15 photocatalysts synthesized through the surface acidolysis of Ti(OnBu)₄ on carboxyl-modified SBA-15. Catal Today. 158:329-335.
- [19] Nadaroglu H, Gungor AA, Celebi N. [2015] Removal of Basic Red 9 (BR9) in Aqueous Solution by Using Silica with Nano-Magnetite by Enzymatic with Fenton Process. International Journal of Environmental Research. 9(3):991-1000.
- [20] Nadaroglu H, Kalkan E, Demir N. [2010] Removal of copper from aqueous solution using red mud. Desalination. 251(1-3):90-95.
- [21] Kalkan E, et al. [2015] Experimental Study to Remediate Acid Fuchsin Dye Using Laccase-Modified Zeolite from Aqueous Solutions. Polish Journal of Environmental Studies. 24(1):115-124.
- [22] Miao SJ, Shanks BH. [2011] Mechanism of acetic acid esterification over sulfonic acid-functionalized mesoporous silica. Journal of Catalysis. 279(1):136-143.
- [23] Vetrivel V, Rajendran K, Kalaiselvi V. [2014-2015] Synthesis and characterization of pure Titanium dioxide nanoparticles by sol- gel method. Int J Chem Tech Res. 7(3):1090-1097.
- [24] Nadaroglu H, et al. [2013] The Evaluation of Affection of Methylo bacterium extorquens - Modified Silica Fume for Adsorption Cadmium (II) Ions from Aqueous Solutions Affection. Kafkas Universities Veteriner Fakultesi Dergisi. 19(3):391-397.
- [25] Saggiaro EM, et al. [2011] Use of Titanium dioxide photocatalysis on the remediation of model textile wastewaters containing azo dyes. Molecules. 16(12):10370-10386.
- [26] Muruganandham M, Sobana N, Swaminathan M. [2006] Solar assisted photocatalytic and photochemical degradation of Reactive Black 5. Journal of Hazardous Materials. 137(3):1371-1376.
- [27] Zielinska B, et al. [2001] Photocatalytic degradation of Reactive Black 5 - A comparison between TiO₂-Tytanpol A11 and TiO₂-Degussa P25 photocatalysts. Applied Catalysis B-Environmental. 35(1): L1-L7.
- [28] Gouvea CAK, et al. [2000] Semiconductor-assisted photocatalytic degradation of reactive dyes in aqueous solution. Chemosphere. 40(4):433-440.
- [29] Yanmis D, et al. [2013] Removal of some textile dyes with laccase from *Anoxybacillus gonensis* (P39). Current Opinion in Biotechnology. 24: S33-S33.
- [30] Daneshvar N, Salari D, Khataee AR. [2003] Photocatalytic degradation of azo dye acid red 14 in water: Investigation of the effect of operational parameters. Journal of Photochemistry and Photobiology a-Chemistry. 157(1):111-116.
- [31] Yesilada O, Cing S, Asma D. [2002] Decolourisation of the textile dye Astrazon Red FBL by *Funalia trogii* pellets. Bioresour Technol. 81(2):155-7.

ARTICLE

AMMONIUM SULPHATE CONCENTRATION OPTIMIZATION AND
ITS RELATION WITH PROTEIN PARAMETERS FOR
CRYSTALLIZATION

Rajneesh K. Gaur

Dept. of Biotechnology, Ministry of Science and Technology, CGO complex, Lodhi Road, New Delhi, INDIA

ABSTRACT



Ammonium sulphate (AS) is the second most utilized precipitant in protein crystallization. This study focused on determining the optimum AS concentration range for crystallizing the four classes of proteins and the relation between the theoretical protein parameters such as isoelectric point and aliphatic index and AS concentration. The data analysis indicates that the AS concentration in 1.5M-2.5M range leads to crystallization of 61.83% of single and soluble proteins and nearly 57% of proteins crystallized as complex structures. In this range, the four classes of proteins show 65.19% (All Alpha), 63.02% (All Beta), 61.09% (Alpha and Beta, $\alpha+\beta$) and 54.27% (Alpha and Beta, α/β) crystallization respectively. There is an inverse relation between theoretical iso-electric Point (pI) and AS conc. facilitates crystallization of 'All Alpha' and 'All Beta' proteins and direct correlation for 'Alpha and Beta' Proteins. It is further observed that there is an inverse relationship between aliphatic index of a protein and AS conc. facilitates crystallization of 'All Alpha' and 'Alpha and Beta' proteins, while correlation is direct for 'All Beta' proteins. These results can be used to improve the existing commercial crystallization screens as well as to predict AS conc. to facilitate crystallization of proteins based on their theoretical isoelectric point and aliphatic index. In conclusion, the optimum ammonium sulphate concentration for crystallization of four classes of proteins is unknown. The data analysis revealed that, in general, ~62% of proteins are crystallized with 1.5M-2.5M of ammonium sulphate concentration range and these results can be used to improve the commercial crystallization screens.

INTRODUCTION

Protein crystallization is a complex phenomenon. In general, protein crystallization is dependent on variety of factors such as precipitant conc. (used either at saturation or in molar quantity), buffer pH & ionic strength and several protein based parameters such as its solubility, isoelectric point, molecular mass, hydrophathy & aliphatic index, etc. [1]. The most successful precipitants for protein crystallization are Polyethylene Glycol (PEG) and Ammonium Sulfate (AS) [2].

The available commercial screens cover sufficient crystallization space while accommodating the precipitant related parameters, buffer PH and salt conc. etc. [3, 4]. In general, number of commercial screens is available; there efficiency of protein crystallization needs improvement through data mining [5]. As a result of statistical analysis, a new crystallization screen called as 'Berkley Screen' is recently available [6].

The data analysis for estimation of PEG types and their conc. in crystallization of various class of protein has been recently reported [7]. Similar study is required for AS as precipitant considering the large number of X-ray based structures is available in the Protein Data Bank (PDB; till date ~124337 protein structures in total). This study is based on data analysis to determine the influence of AS concentration on different classes of single & soluble protein crystallization and the related protein parameters. The outcome of the study will be helpful in improving the efficiency of available AS crystallization screens or formulating new screens as well as to predict the AS conc. for crystallizing a particular class of protein utilizing the theoretical parameters of a protein sequence.

METHODS

The soluble proteins crystallized with Ammonium Sulphate (AS) and having 30% sequence identity are downloaded from Protein Data Bank (PDB) [8]. Out of the 1062 downloaded X-ray diffracted protein entries, only 162 protein entries are used in experimental dataset. The number of membrane protein entries is insufficient for data analysis. The protein entries are curated after excluding the entries crystallized in complex with any type of ligand including protein/peptide/any chemical entity such as ATP, FAD etc. and those possess inadequate and insufficient crystallographic information. Only the non-redundant crystallization conditions were incorporated in the experimental dataset. For analytical purpose, the experimental dataset of soluble proteins is further divided into four sub-datasets of 'All Alpha (28)', 'All Beta (50)', 'Alpha and Beta [a/b (39); a+b (45)]' proteins as per the Structural Classification of Protein (SCOP) [9]. The percentage of proteins crystallized at a particular Ammonium Sulphate Concentration is manually calculated. The theoretical protein parameters i.e. isoelectric point and Aliphatic index are calculated by using 'Prot Param' tool available on Expsy server [10] and the entire data is analyzed manually.

KEY WORDS

Ammonium Sulphate (AS) Concentration, Protein Crystallization, Isoelectric point, Aliphatic index

Received: 23 March 2018
Accepted: 25 May 2018
Published: 8 Aug 2016

*Corresponding Author

Email: meetgaur@gmail.com
Tel.: +11-24362982
Fax: +11-24360745

RESULTS AND DISCUSSION

Ammonium Sulphate (AS) and PEG are the two main precipitant used for protein crystallization. This study is focused on AS concentration (M) determination facilitating the maximum percentage of various classes of soluble protein crystallization and its relation with two theoretical protein parameters i.e. iso electric point & Aliphatic index. Earlier also the AS concentration optimization for protein crystallization has been reported [11].

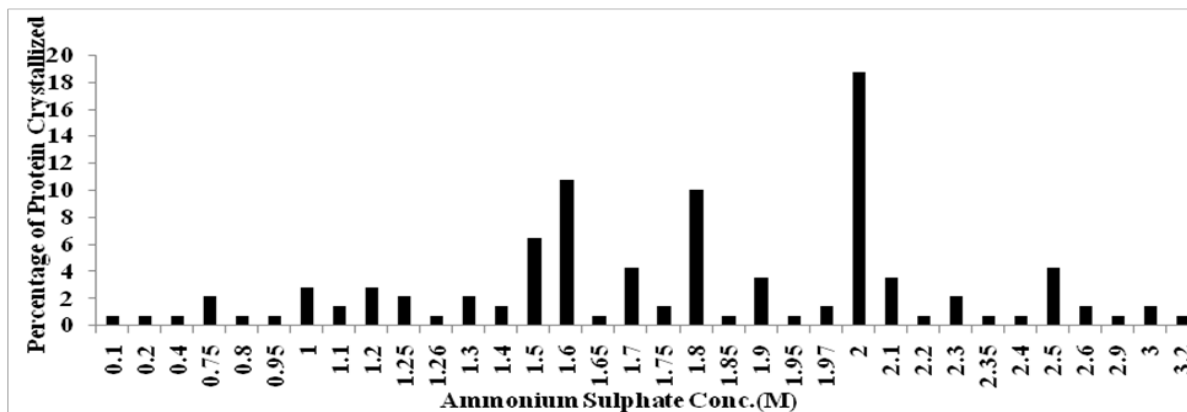


Fig. 1: Shows the percentage of soluble proteins crystallized with different Ammonium Sulphate Concentrations (M).

In last few years, there is a tremendous growth in PDB database of protein structures crystallized through X-ray diffraction method, therefore, it is pertinent to determine the optimized AS concentration for protein of various classes. As a result, an experimental dataset of soluble single proteins having 30% sequence identity was prepared and subdivided in to four subsets i.e. 'All Alpha', 'All Beta', Alpha and Beta (alpha/beta & alpha+ Beta). The manual analysis of the overall dataset revealed that the AS concentration in decreasing order of 2M>1.6M>1.8M>1.5M facilitated the percentage crystallization of soluble proteins [Fig. 1]. These four AS concentrations leads to the crystallization of 46.03% of proteins in total and 18.7%>10.79%>10.07%>6.47% independently. In addition, the AS concentration each of 1.7M, 1.9M, 2.1M & 2.5M results in crystallization of 4.31%, 3.59% & 4.31% of proteins independently, which cumulatively leads to 15.8% of protein in total. Therefore, the range of AS concentration leading to crystallization of 61.83% of single soluble proteins is 1.5M-2.5M. In market, number of commercial kits is available such as Ammonium Sulphate suite (Qiagen, Germany) & Grid Screen AS (Hampton Research, USA). In these commercially available screens, the AS concentration used either in multiple of a particular concentration such as multiples of 0.8M AS is used in Grid Screens (Hampton Research) or use of a particular concentration in majority of conditions such as 2.2M in Ammonium Sulphate Suite (Qiagen). In contrast to the deduced AS Conc. range, the existing commercial screens using extremes of AS Conc. However, the AS conc. range of 1.5M to 2.5M if included at an interval of 0.2M in available commercial AS screens might enhance their efficiency.

Table 1. Shows the Ammonium Sulphate (AS) Concentration (M) and percentage of four classes of single and soluble protein crystallized at 5% or above AS conc.

Ammonium Sulphate concentration (M)	Protein Classes (as per SCOP classification)			
	All Alpha	All Beta	Alpha and Beta (α/β)	($\alpha+\beta$)
2.5	-	5.16	5.71	-
2.0	21.73	15.78	20.0	22.22
2.1	8.69	7.89	-	-
1.9	-	-	5.71	5.55
1.8	17.39	7.89	8.57	11.11
1.7	-	5.26	-	5.55
1.6	8.69	13.15	14.28	8.33
1.5	8.69	7.89	-	8.33
1.3	-	5.26	-	-
1.2	-	5.26	-	-
1.1	-	-	-	5.55
1.0	-	-	5.71	-
0.75	8.69	-	-	-

Further, the AS concentration resulting in the crystallization of four classes of proteins crystallized was studied [Fig. 2]. The results show that all the four protein classes show the maximum crystallization percentage at three AS conc of 2.0M>1.8M>1.6M [Table 1]. All the protein classes show highest percentage of crystallization at 2.0M AS conc. However, 'All Alpha' and 'Alpha and Beta ($\alpha+\beta$)' shows higher percentage of crystallization at 1.8M AS conc. in comparison to 'All Beta' and 'Alpha & Beta (α/β)' proteins. These classes show higher crystallization percentage at 1.6M AS conc. in comparison to 'All Alpha' and 'Alpha and Beta ($\alpha+\beta$)' class of proteins. These four classes of proteins show 36-47% of crystallization percentage at three AS conc. i.e. 2.0M, 1.8M and 1.6M. 'Alpha and Beta (α/β & $\alpha+\beta$)' protein class show similar percentage of crystallization i.e. ~42%, while 'All Alpha (47.81%)' & 'All Beta (36.82%)' proteins remains at two extreme at these three AS conc. It may be due to the fact that the alpha-helix structure is determined by tertiary structure and beta sheets by intrinsic properties of the residues in the strand [12]. In alpha helices, the tertiary structure formation involves variation of amino acid residues, while beta sheet residues are more conserved [13]. Beta sheets are stabilized by hydrophobic contacts and backbone hydrogen bonding. Alpha helices are largely stabilized by backbone H-bonding i.e. local interactions dominate in a Helix, whereas a sheet is stabilized by long range contacts. So, any disturbance of hydrophobic bonds in Beta sheets could result in exposure of hydrophobic residues and leading to difficulty in crystallization. Therefore, low value for 'All Beta' proteins. Furthermore, though the residues in beta sheets are conserved, possibly the existence of high mobility of folds or other inconsistent secondary structures is not allowing the crystallization of high percentage of 'All Beta' proteins, while the alpha-helices in 'All-Alpha' proteins possess greater flexibility to accommodate such disturbances due to better protein-protein/water interaction and leading to high percentage of protein crystallization of 'All-Alpha' proteins at these three AS conc. The observed difference in AS conc. in 'Alpha and Beta' class of protein crystallization is due to the proportional difference of Helices & Beta Sheets in this class of protein, which leading to various levels of repulsive protein-protein interactions [14].

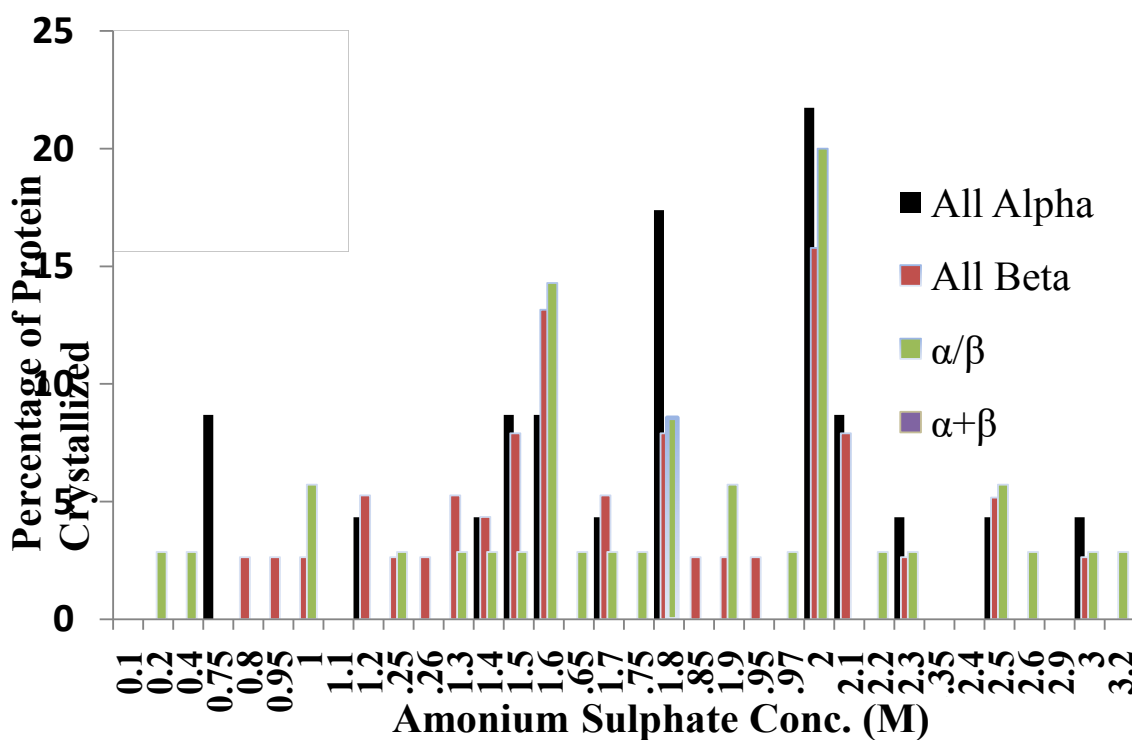


Fig. 2: Shows the percentage of various classes of soluble proteins crystallized with different Ammonium Sulphate Concentrations (M). The different classes of proteins are All Alpha (Black), All Beta (Maroon), Alpha and Beta (α/β - Green & $\alpha+\beta$ - Purple).

An interesting observation is that four classes of proteins show 65.19% (All Alpha), 63.02% (All Beta), 61.09% (Alpha and Beta, $\alpha+\beta$) and 54.27% (Alpha and Beta, α/β) percentage crystallization respectively within the AS conc. range of 1.5M-2.5M [Fig. 2]. Exceptionally, 'All Alpha (8.69%)' proteins also show good chances of crystallization at 0.75M. These results suggest significant percentage of the four classes of proteins is crystallized within a narrow AS conc. range of 1.5M-2.5M. Therefore, the narrow AS conc. range can be utilized to formulate new commercial screens for minimizing the wastage of precious protein samples and to obtain the crystallization conditions quickly. In addition, the new screens can also accommodate a separate slot at 0.75M AS conc. to enhance the crystallization efficiency for 'All Alpha' class of proteins. High throughput platforms or Structural Consortia provide ample scope to experimentally validate these results for single and soluble proteins, whose structures are not yet available.

Table 2. The Ammonium Sulphate (AS) Concentration (M) and percentage of four classes of protein crystallized at 5% or above AS conc. as complex

Ammonium Sulphate concentration (M)	Protein Classes (as per SCOP classification)			
	All Alpha	All Beta	Alpha and Beta (α/β)	Alpha and Beta ($\alpha+\beta$)
3.5	6.66	9.52	-	-
3.2	6.66	-	-	-
2.9	6.66	-	-	-
2.8	-	-	-	9.52
2.5	13.33	-	-	-
2.4	-	-	5.26	-
2.2	13.33	-	-	-
2.1	-	-	5.26	9.52
2.0	6.66	33.33	21.05	23.80
1.9	-	-	7.89	-
1.8	6.66	19.04	5.26	14.28
1.7	13.33	-	-	-
1.6	6.66	-	7.89	-
1.5	-	-	10.52	19.04
1.4	6.66	-	5.26	-
1.3	-	-	5.26	-
1.2	-	9.52	10.52	-
1.1	-	-	-	-
1.0	-	-	-	-
0.9	-	-	5.26	-
0.75	-	-	-	-
0.20	6.66	-	-	-

Furthermore, the AS concentration resulting in the crystallization of four classes of proteins as complex structures was studied as only limited data for unique complex structures is available. The dataset includes only the protein complex entries having 30% sequence identity to accommodate the maximum available pool of distinct protein sequences/structures. The analysis indicates that the AS conc. leading to crystallization of proteins as complex structures showed a preferential pattern. The three protein classes as complex structures show the maximum crystallization percentage at 2.0M and a preferential pattern at other AS concentrations [Table 2]. 'All Alpha' proteins class as complex structures show a distinct preference at 1.7M, 2.2M & 2.5M leading to crystallization of approx. 40% of 'All Alpha' proteins as complex structures. 'All Beta' proteins class as complex structure show a distinct preference for only four AS conc. in an order of 2.0M>1.8M>1.2M=3.5M. It indicates that nearly 50% of 'All Beta' proteins crystallized as complex at only narrow range of two AS conc. i.e. 2.0M (33.33%) & 1.8M (19.04%). 'Alpha and Beta ($\alpha+\beta$)' proteins class as complex structures shows preference in an order of 2.0M>1.5M>1.8M>2.8M. 'Alpha and Beta (α/β)' proteins class as complex structures shows preference in an order of 2.0M>1.5M=1.2M>1.6=1.9M>1.3M=1.4M=2.1M=2.4M=0.9M. 'Alpha and Beta ($\alpha+\beta$ & α/β)' protein classes show maximum crystallization as complex at three AS concentration. Alpha and Beta ($\alpha+\beta$)' protein class shows 57.12% of crystallization as complex at three AS conc. i.e. 2.0M (23.80%)>1.5M (19.04%)>1.8M (14.28%). Alpha and Beta (α/β)' protein class shows 42.09% of crystallization as complex at three AS conc. i.e. 2.0M (21.05%)>1.5M (10.52%) =1.2M (10.52%) class of proteins. These four classes of proteins show 36-47% of crystallization percentage at three AS conc. i.e. 2.0M, 1.8M and 1.6M. 'Alpha and Beta (α/β & $\alpha+\beta$)' protein class show similar percentage of crystallization i.e. ~42%, while 'All Alpha (47.81%)' & 'All Beta (36.82%)' proteins remains at two extreme at these three AS conc. The preferential pattern observed for the four protein classes as complex structures is influenced by type and chemical nature of the lig and/substrate/inhibitor/protein etc. and the resulting interplay of attractive and repulsive forces due to exposure of acidic and/or basic protein surface residues. In spite of a preferential pattern for AS conc. is observed, broadly it can be concluded that the optimum AS conc. leading to crystallization of all the four classes of proteins as complex structures lie within a narrow range of 1.5M-2.5M as also observed above in case of single & soluble proteins. Therefore, this narrow AS conc. range can be utilized in the preparation of commercial screens having improved crystallization efficiency with lower protein requirement.

The two theoretical protein parameters i.e. iso-electric point (pI) and aliphatic index studied for the four classes of single & soluble proteins in order to understand the correlation between these protein parameters and AS conc. facilitated the crystallization of proteins. This study is not followed for complex structure as these are protein sequence based parameters. These two protein parameters are considered as there is an increased chance for a protein to crystallize near the pI of the protein moiety [15] and Aliphatic index is an indicator of thermo stability of a protein [16] and also used to predict the interaction with other molecules or surfaces, which might influence the AS conc. based crystallization of proteins. The results shows an inverse relation between iso-electric Point (pI) and AS conc. for 'All Alpha' and 'All Beta' proteins and direct correlation for 'Alpha and Beta' Proteins [Fig. 3, 4, 5, 6]. In case of 'All Alpha' and 'All Beta' proteins, the protein crystallizes at lower AS conc. with increase of iso-electric point of a protein. The overall slope of the two curves does not show a sudden change, though there is a noticeable difference

between the slope of the curve for 'All Alpha & All Beta' proteins. 'Alpha and Beta' proteins correlation curve shows that with increase of iso-electric point there is an increase of AS conc. requirement for crystallization of these classes of proteins. The slope of the curve is more acute in case of α/β proteins in comparison to $\alpha+\beta$ proteins. These results are in contrast as reported earlier for ovalbumin (an alpha & beta protein). These contrasting results are possibly due to the fact that in ovalbumin publication, there is an inverse correlation between ionic strength of a buffer and iso-electric point of a protein [17].

The curves between aliphatic index of a protein and AS conc. shows that the 'All Alpha' and 'Alpha and Beta' proteins possess inverse relationship, while 'All Beta' proteins possess direct correlation between the two parameters [Fig. 7, 8, 9, 10]. The slope of the curve is more acute in case of 'Alpha and Beta Proteins'.

The smooth steepness of the curve observed for AS conc. facilitated crystallization of four classes of proteins and iso-electric point/Aliphatic index of the proteins is due to the narrow range of AS conc. leading to protein crystallization.

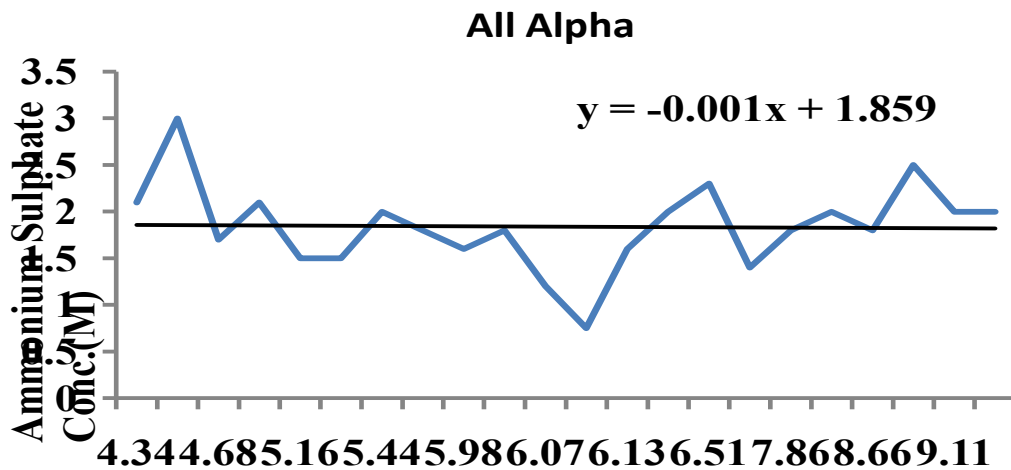


Fig. 3: Shows the relation between Iso-electric point (pI) and Ammonium Sulphate (AS) Concentration (M) for Alpha Protein type. The Graph also shows the trend line equation.

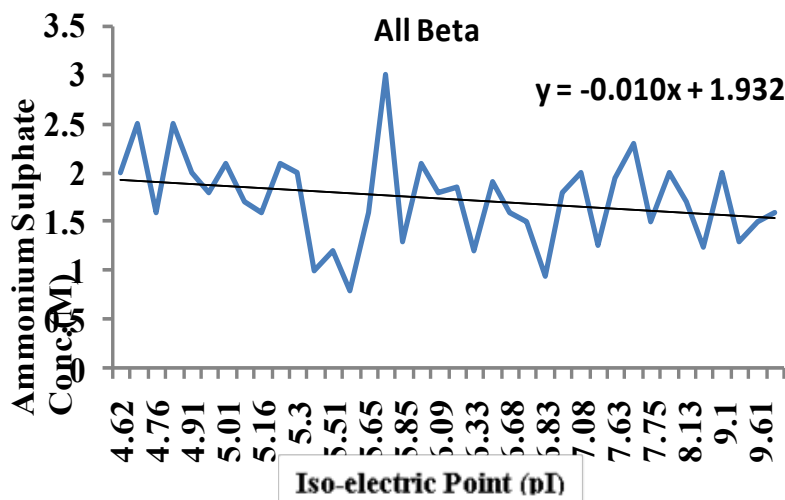


Fig. 4: Shows the relation between Iso-electric point (pI) and Ammonium Sulphate (AS) Concentration (M) for Beta Protein type. The Graph also shows the trend line equation.

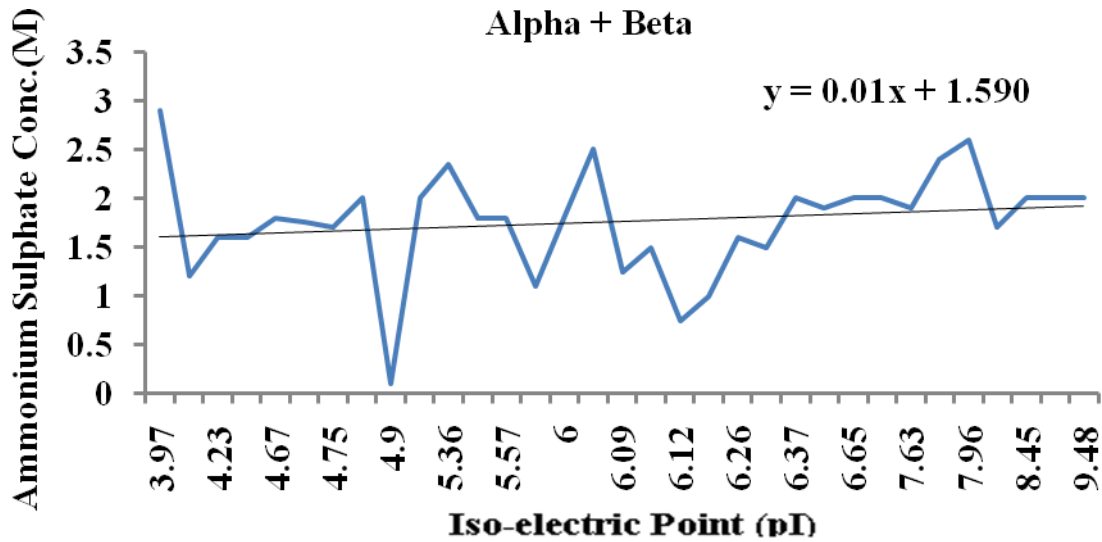


Fig. 5: Shows the relation between Iso-electric point (pI) and Ammonium Sulphate (AS) Concentration (M) for Alpha and Beta (α+β) Protein type. The Graph also shows the trendline equation.

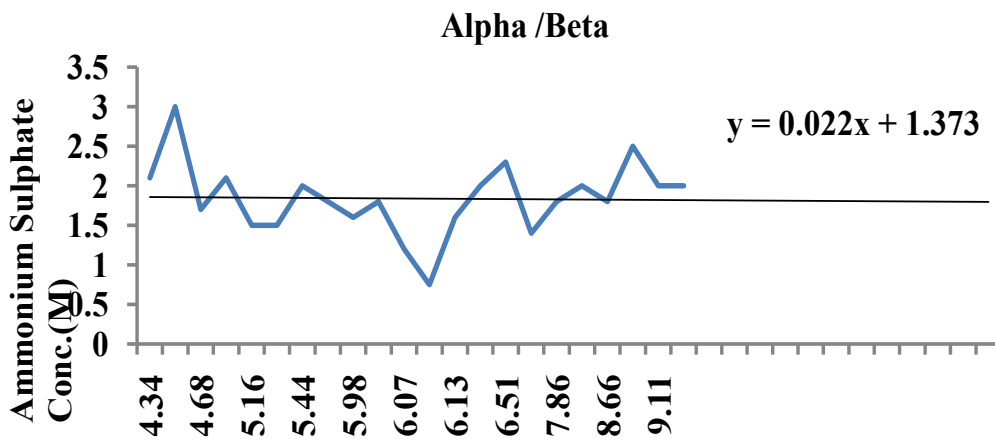


Fig. 6: Shows the relation between Iso-electric point (pI) and Ammonium Sulphate (AS) Concentration (M) for Alpha and Beta (α/β) Protein type. The Graph also shows the trendline equation.

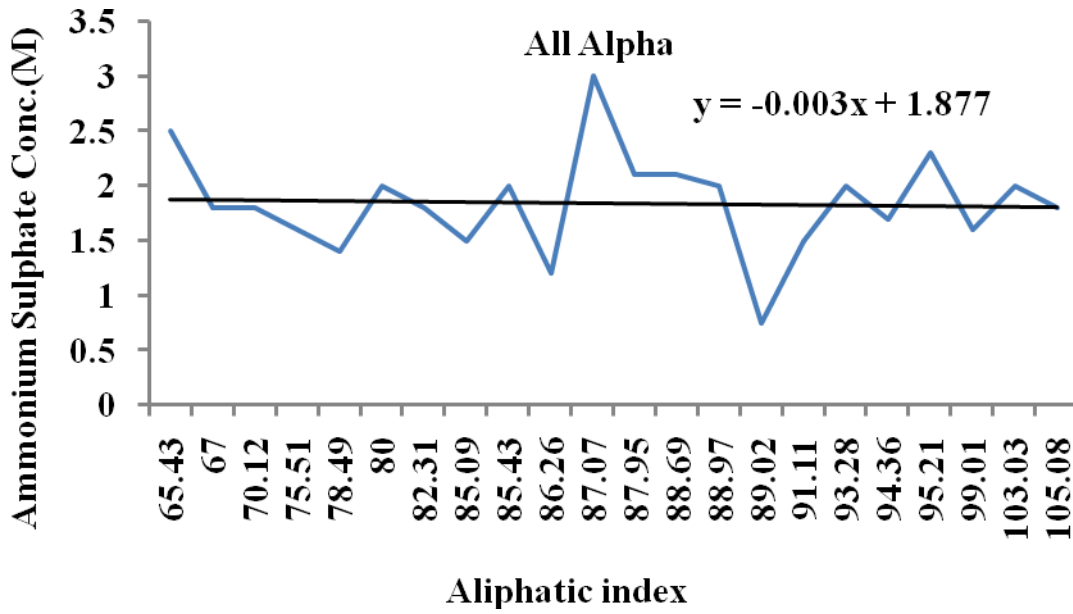


Fig. 7: Shows the relation between Aliphatic Index and Ammonium Sulphate (AS) Concentration (M) for Alpha Protein type. The Graph also shows the Trendline equation.

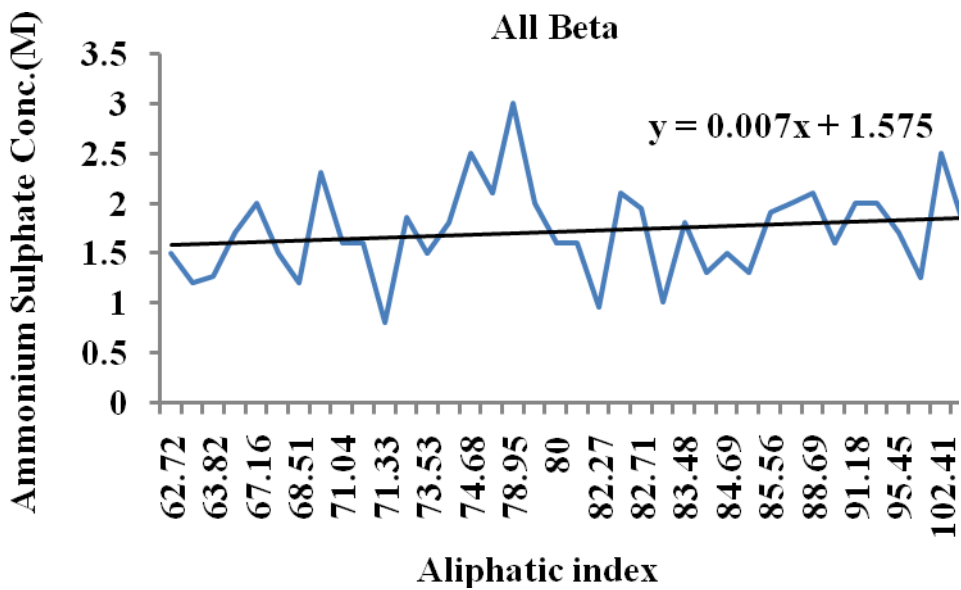


Fig. 8: Shows the relation between Aliphatic Index and Ammonium Sulphate (AS) Concentration (M) for Beta Protein type. The Graph also shows the trendline equation.

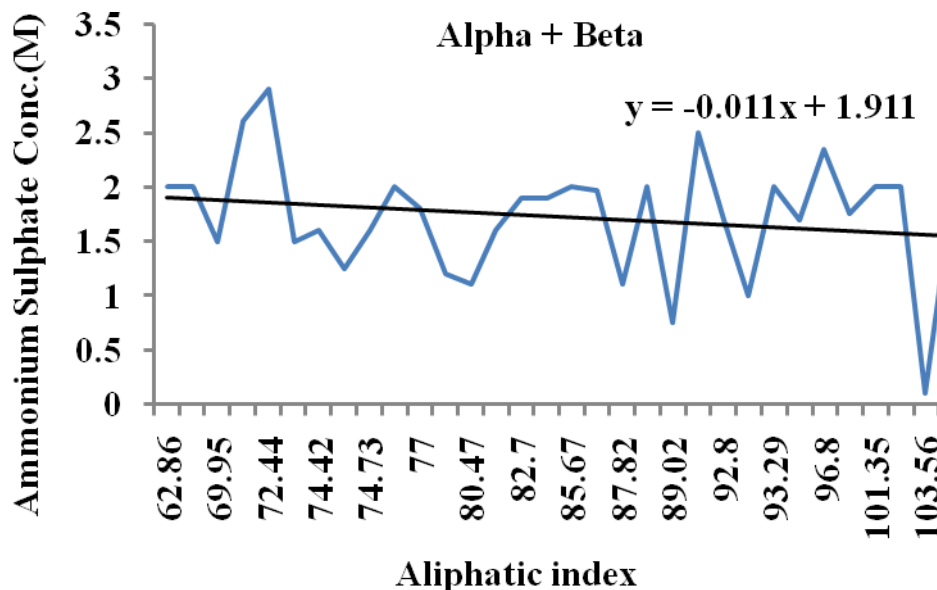


Fig. 9: Shows the relation between Aliphatic Index and Ammonium Sulphate (AS) Concentration (M) for Alpha and Beta ($\alpha+\beta$) Protein type. The Graph also shows the trendline equation.

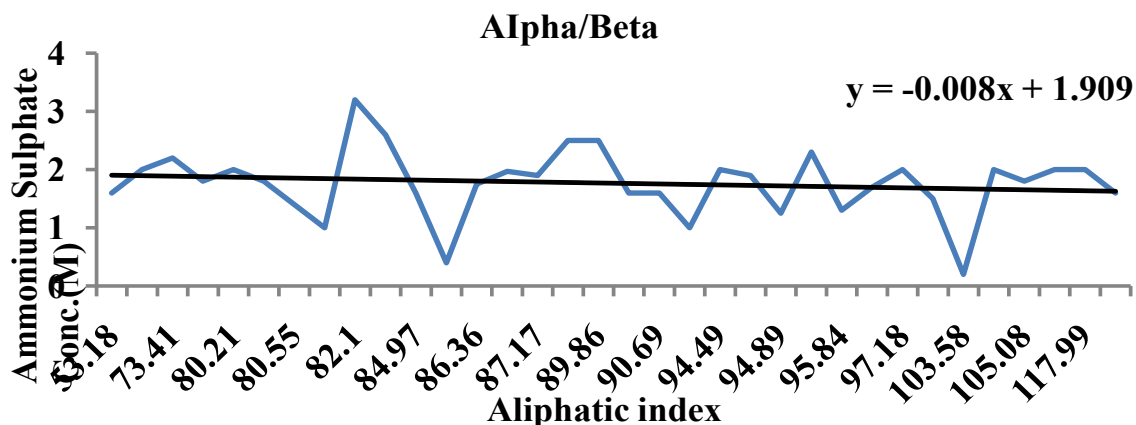


Fig. 10: Shows the relation between Aliphatic Index and Ammonium Sulphate (AS) Concentration (M) for Alpha and Beta (α/β) Protein type. The Graph also shows the trendline equation.

CONCLUSION

A number of AS based commercial screens are available and there is a scope of improving the efficiency of these screens. These results indicate that substantial percentage of four classes of proteins is crystallized within a narrow range of AS conc. i.e. 1.5-2.5M. Further the curves deduced between the two theoretical protein parameters i.e. isoelectric point and Aliphatic index and AS conc. suggest that these curves may be used as reference curves for determining the AS conc., which may facilitate protein crystallization for a particular class. Indeed, these results need empirical validation for improving the efficiency of crystallization process.

CONFLICT OF INTEREST

The author declares having no competing interest.

ACKNOWLEDGEMENTS

None

FINANCIAL DISCLOSURE

No Funding agency supported the study.

ABBREVIATIONS: PEG –Polyethylene Glycol, AS – Ammonium Sulphate

REFERENCES

- [1] McPherson A. [1999] Crystallization of Biological Macromolecules. Cold Spring Harbor Laboratory Press, Cold Spring Harbor, NY.
- [2] Dumetz AC, Chockla AM, Kaler EW, Lenhoff AM. [2009] Comparative Effects of Salt, Organic, and Polymer Precipitants on Protein Phase Behavior and Implications for Vapor Diffusion Growth Des 9: 682-691.
- [3] Page R, Stevens RC. [2004] Crystallization data mining in structural genomics: using positive and negative results to optimize protein crystallization screens Methods. 34: 373-389.
- [4] Newman J, Egan D, Walter TS, et al. [2005] Towards rationalization of crystallization screening for small- to medium-sized academic laboratories: the PACT/JCSG+ strategy, Acta Cryst D. 61: 1426-1431.
- [5] Luft JR, Newman J, Snell EH. [2014] Crystallization screening: the influence of history on current practice, Acta Cryst F Struct Biol Comm. 70(7):835-853.
- [6] Pereira JH, McAndrew RP, Tomaleri GP, Adams PD. [2017] Berkeley Screen: a set of 96 solutions for general macromolecular crystallization. J Appl Cryst. 50(5):1352-1358.
- [7] Gaur RK. [2016] Estimation of PEG types and their concentration during protein crystallization. The IIOAB J 7(7):5-9
- [8] Berman HM, Westbrook J, Feng Z, et al. [2000] The protein Data Bank Nucleic Acids Res 28:235–242.
- [9] Murzin AG, Brenner SE, Hubbard T, Chothia C. [1995] SCOP: a structural classification of proteins database for the investigation of sequences and structures J Mol Biol 247:536-540
- [10] Gasteiger E, Hoogland C, et al. [2005] Protein Identification and Analysis Tools on the ExPASy Server; John M Walker (ed): The Proteomics Protocols Handbook, Humana Press 571-607.
- [11] McPherson A. [1990] Current approaches to macromolecular crystallization. Eur J Biochem 189:1-23.
- [12] Minor DI Jr, Kim PS. [1994] Context is a major determinant of Beta sheet propensity, Nature 371(6494):264-267.
- [13] Sitbon E, Pietrokovski S. [2007] Occurrence of Protein Structure Elements in conserved sequence regions. BMC Struct Biol 7:3.
- [14] Dumetz AC, Sneelinger O'Brien AM, Kaler EW, Lenhoff AM. [2007] Patterns of Protein-Protein interactions in Salt solutions and implication for Protein crystallization, Prot Sci 16:1867-1877.
- [15] Kantardjieff KA, Rupp B. [2004] Protein isoelectric point as a predictor for increased crystallization screening efficiency Bioinf 20:2162-2168.
- [16] Ikai A. [1980]. Thermo stability and aliphatic index of globular proteins, J Biochem. 88:1895-1898.
- [17] Smith ERB. [1935] The effect of variations in ionic strength on the apparent isoelectric point of egg albumin, J Biol Chem. 108:187-194.